

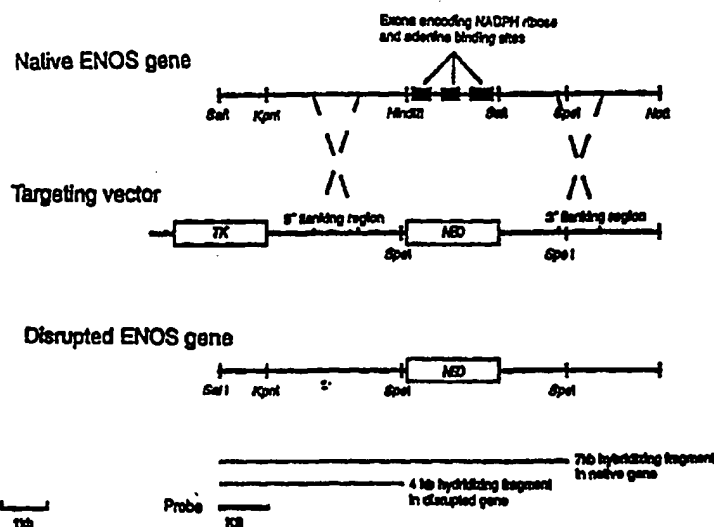


PCT

WORLD INTELLECTUAL PROPERTY ORGANIZATION  
International Bureau

## INTERNATIONAL APPLICATION PUBLISHED UNDER THE PATENT COOPERATION TREATY (PCT)

<b>(51) International Patent Classification <sup>6</sup>:</b> <b>C12N 15/00, A01K 67/027, C12N 9/02, 15/53</b>	<b>A1</b>	<b>(11) International Publication Number:</b> <b>WO 97/33989</b> <b>(43) International Publication Date:</b> 18 September 1997 (18.09.97)
<b>(21) International Application Number:</b> PCT/US97/04184 <b>(22) International Filing Date:</b> 14 March 1997 (14.03.97)  <b>(30) Priority Data:</b> 60/013,525      15 March 1996 (15.03.96)      US 60/027,362      18 September 1996 (18.09.96)      US  <b>(71) Applicant:</b> THE GENERAL HOSPITAL CORPORATION [US/US]; Fruit Street, Boston, MA 02114 (US).  <b>(72) Inventors:</b> HUANG, Paul, L.; 18 Temple Street, Boston, MA 02114 (US). FISHMAN, Mark, C.; 43 Kenwood Avenue, Newton Center, MA 02159 (US). MOSKOWITZ, Michael, A.; 275 Prospect Street, Belmont, MA 02178 (US).  <b>(74) Agents:</b> GOLDSTEIN, Jorge, A. et al.; Sterne, Kessler, Goldstein & Fox P.L.L.C., Suite 600, 1100 New York Avenue, N.W., Washington, DC 20005-3934 (US).		<b>(81) Designated States:</b> CA, JP, MX, European patent (AT, BE, CH, DE, DK, ES, FI, FR, GB, GR, IE, IT, LU, MC, NL, PT, SE).  <b>Published</b> <i>With international search report.</i> <i>Before the expiration of the time limit for amending the claims and to be republished in the event of the receipt of amendments.</i>

**(54) Title:** TRANSGENIC ANIMALS HAVING A DISRUPTED eNOS GENE AND USE THEREOF**(57) Abstract**

This invention relates to transgenic non-human animals comprising a disrupted endothelial nitric oxide synthase gene. These animals exhibit abnormal wound-healing properties and hypertension. This invention also relates to methods of using the transgenic animals to screen for compounds having a potential therapeutic utility for vascular endothelial disorders, such as hypertension, cerebral ischemia or stroke, atherosclerosis and wound-healing activities. Moreover, this invention also relates to methods of treating a patient suffering from hypertension and wound-healing abnormalities with the compounds identified using the transgenic animals, and methods of making the transgenic animals. A method of treating a wound using nitroglycerin is also provided.

BEST AVAILABLE COPY

**FOR THE PURPOSES OF INFORMATION ONLY**

Codes used to identify States party to the PCT on the front pages of pamphlets publishing international applications under the PCT.

AM	Armenia	GB	United Kingdom	MW	Malawi
AT	Austria	GE	Georgia	MX	Mexico
AU	Australia	GN	Guinea	NE	Niger
BB	Barbados	GR	Greece	NL	Netherlands
BE	Belgium	HU	Hungary	NO	Norway
BF	Burkina Faso	IE	Ireland	NZ	New Zealand
BG	Bulgaria	IT	Italy	PL	Poland
BJ	Benin	JP	Japan	PT	Portugal
BR	Brazil	KE	Kenya	RO	Romania
BY	Belarus	KG	Kyrgyzstan	RU	Russian Federation
CA	Canada	KP	Democratic People's Republic of Korea	SD	Sudan
CF	Central African Republic	KR	Republic of Korea	SE	Sweden
CG	Congo	KZ	Kazakhstan	SG	Singapore
CH	Switzerland	LI	Liechtenstein	SI	Slovenia
CI	Côte d'Ivoire	LK	Sri Lanka	SK	Slovakia
CM	Cameroon	LR	Liberia	SN	Senegal
CN	China	LT	Lithuania	SZ	Swaziland
CS	Czechoslovakia	LU	Luxembourg	TD	Chad
CZ	Czech Republic	LV	Latvia	TG	Togo
DE	Germany	MC	Monaco	TJ	Tajikistan
DK	Denmark	MD	Republic of Moldova	TT	Trinidad and Tobago
EE	Estonia	MG	Madagascar	UA	Ukraine
ES	Spain	ML	Mali	UG	Uganda
FI	Finland	MN	Mongolia	US	United States of America
FR	France	MR	Mauritania	UZ	Uzbekistan
GA	Gabon			VN	Viet Nam

**Transgenic animals having a disrupted eNOS gene and use thereof*****Background of the Invention******Statement as to Rights to Inventions Made Under  
Federally-Sponsored Research and Development***

5

Part of the work performed during the development of this invention was supported by U.S. Government funds. The U.S. Government may have certain rights in this invention.

***Field of the Invention***

10

This invention relates to transgenic non-human animals comprising a disrupted endothelial nitric oxide synthase gene. This invention also relates to methods of using these transgenic animals to screen compounds for activity against vascular endothelial disorders such as hypertension, stroke, and atherosclerosis, as well as for wound healing activity; methods of treating a patient suffering from a vascular endothelial disorder; methods of making the transgenic animals; and cell lines comprising a disrupted eNOS gene.

15

***Related Art***

In 1980, Furchgott and Zawadzki first proposed the existence of endothelium derived relaxing factor or EDRF, later identified as nitric oxide. Furchgott (1980); Furchgott (1988); Ignarro (1988); Palmer (1987). Nitric oxide is an important messenger molecule produced by endothelial cells, neurons, macrophages, and other tissues. Marletta (1989); Moncada (1991); Nathan (1992); Snyder (1992); and Dawson *et al.* (1992). Since nitric oxide is a gas with no known storage mechanism, it diffuses freely across membranes and is extremely labile. Nitric oxide has a biological half-life on the order of seconds.

20

25

-2-

Nitric oxide exhibits several biochemical activities. This compound can bind to and activate soluble guanyl cyclase, resulting in increased cGMP levels. Nitric oxide also modifies a cysteine residue in glyceraldehyde-3-phosphate dehydrogenase by adenosine diphosphate ribosylation, Zhang & Snyder (1992), Katz *et al.* (1992), and Dimmeler *et al.* (1992), or S-nitrosylation via NAD interactions, McDonald & Moss (1993). Nitric oxide also binds to a variety of iron- and sulphur-containing proteins, Marletta (1993), and may have other modes of action as well.

Nitric oxide formation is catalyzed by the nitric oxide synthase enzymes (NOS). These enzymes act by producing nitric oxide from the terminal guanidino nitrogen of arginine, with the stoichiometric production of citrulline. There are several NOS isoforms encoded by separate genes. Marletta (1993), and Lowenstein & Snyder (1992). The various NOS isoforms are about 50-60% homologous overall. Some forms of NOS are found in most tissues. The different NOS isoforms: neuronal NOS (nNOS), macrophage NOS (iNOS), and endothelial NOS (eNOS), are now known as type I NOS, type II NOS and type III NOS, respectively. The properties of these NOS isoforms are summarized in the following Table:

Property	Type I NOS	Type II NOS	Type III NOS
Common name	nNOS	iNOS	eNOS
Typical cell	neurons	macrophages	endothelium
Other sites of expression	smooth muscle	endothelium smooth muscle	smooth muscle neurons
Expression	constitutive	inducible	constitutive
Regulation	Ca/CaM	transcription	Ca/CaM
Output	moderate (nM to $\mu$ M)	high ( $\mu$ M)	low (pM to nM)
Function	signalling	toxin	signalling

The ubiquitous presence of blood vessels and nerves means that the endothelial and neuronal isoforms may be present in most tissues. The expression of the endothelial and neuronal isoforms can also be induced in cells that normally do not express them. The sequence of these isoforms have been published or are available in Genbank under the following accession numbers:

Gene:	Species:			
	Man	Rat	Mouse	Cow
<b>Neuronal (type I)</b>	U17327	X59949	D14552	
	D16408			
	L02881			
<b>Macrophage (type II)</b>	L09210	D14051	M87039	U18331
	X85759-81	D83661	U43428	U14640
	U18334	U26686	L23806	
	U31511	U16359	L09126	
	U20141	D44591	M92649	
	U05810	X76881	M84373	
	X73029	U02534		
	L24553	L12562		
<b>Endothelial (type III)</b>	X76303-16	U18336		M89952
	L26914	U28933		L27056
	L23210			M95674
	L10693			M99057
	M95296			M89952
	M93718			

Each of these sequences are expressly incorporated herein by reference.

In blood vessels, the endothelial NOS isoform mediates endothelium-dependent vasodilation in response to acetylcholine, bradykinin, and other mediators. Nitric oxide also maintains basal vascular tone and regulates regional

blood flow. Nitric oxide levels increase in response to shear stress, i.e., forces on the blood vessels in the direction of blood flow, and to mediators of inflammation. Furchgott & van Houtte (1989); Ignarro (1989).

In the immune system, the macrophage isoform is produced by activated  
5 macrophages and neutrophils as a cytotoxic agent. Nitric oxide produced in these cells targets tumor cells and pathogens. Hibbs *et al.* (1988); Nathan (1992); and Marletta (1989).

In the nervous system, the neuronal NOS isoform is localized to discrete  
10 populations of neurons in the cerebellum, olfactory bulb, hippocampus, cortex, striatum, basal forebrain, and brain stem. Bredt *et al.* (1990). NOS is also concentrated in the posterior pituitary gland, in the superoptic and paraventricular hypothalamic nuclei, and in discrete ganglion cells of the adrenal medulla. *Id.* The widespread cellular localization of neuronal NOS and the short half-life and  
15 diffusion properties of nitric oxide suggest that it plays a role in nervous system morphogenesis and synaptic plasticity.

During development, NO may influence activity-dependent synaptic  
pruning, apoptosis, and the establishment of the columnar organization of the  
cortex. Gally *et al.* (1990), Edelman & Gally (1992). Two forms of long-term  
synaptic modulation, long-term depression of the cerebellum, Shibuki & Okada  
20 (1991), and long-term potentiation (LTP) in the hippocampus, are sensitive to inhibitors of NOS. Bohme *et al.* (1991); Haley *et al.* (1992); O'Dell *et al.* (1991); Schuman & Madison (1991). Thus, nitric oxide may serve as a retrograde neurotransmitter to enhance synaptic function due to correlated firing of pre-and  
postsynaptic cells.

In the peripheral nervous system, nitric oxide mediates relaxation of  
25 smooth muscle. Smooth muscle relaxation in the gut, important to adaptation to a bolus of food and peristalsis, depends upon inhibitory non adrenergic, noncholinergic nerves that mediate their effects via nitric oxide. Boeckstaens  
*et al.* (1991); Bult *et al.* (1990); Desai *et al.* (1991); Gillespie *et al.* (1989);  
30 Gibson *et al.* (1990); Ramagopal & Leighton (1989); Tottrup *et al.* (1991). NOS-

containing neurons also innervate the corpus carvornosa of the penis, Burnett *et al.* (1992); Rajfer *et al.* (1992), and the adventitial layer of cerebral blood vessels. Nozaki *et al.* (1993); Toda & Okamura (1990). Stimulation of these nerves can lead to penile erection and dilation of cerebral arteries, respectively. These effects are blocked by inhibition of NOS.

Various biological roles of NO are described by Schmidt & Walter (1994); Nathan & Xie (1994); and Snyder (1995). The major roles of nitric oxide include:

- (1) vasodilation or vasoconstriction with resulting change in blood pressure and blood flow;
- (2) neurotransmission in the central and peripheral nervous system, including mediation of signals for normal gastrointestinal motility; and
- (3) defense against pathogens like bacteria, fungus, and parasites due to the toxicity of high levels of NO to pathogenic organisms.

Recently, a role for NO has been proposed in the pathophysiology of cerebral ischemia, one form of vascular endothelial disorder. Iadecola *et al.* (1994); Dalkara and Moskowitz (1994). Since NO is diffusible, short-lived, and reactive free radical gas that is difficult to measure *in vivo*, Archer (1993), most studies examining ischemic outcomes have based their conclusions on results following NOS inhibition by arginine analogues such as nitro-L-arginine or nitro-L-arginine methyl ester. These inhibitors, however, lack enzyme selectivity and block multiple isoforms. Rees *et al.* (1990). This nonselectivity might account in part for the discrepant outcomes after administration of NOS inhibitors following middle cerebral artery (MCA) occlusion.

Atherosclerosis is another form of a vascular endothelial disorder. This disease, a major cause of morbidity and mortality, is progressive beginning many years before the onset of overt symptoms. During the development of atherosclerosis, biochemical, cellular, and hemodynamic forces drive change in blood vessel walls, which ultimately leads to endothelial dysfunction, cellular proliferation, recruitment of endothelial cells, and accumulation of oxidized LDL.

Ross (1995). The cellular and molecular mechanisms that underlie these processes are complex. Rodent models offer the ability to study the contribution of individual genes, alone or in combination, to the molecular events in atherosclerosis. Breslow (1996); Ross (1996).

5           Cells within atherosclerotic plaques are monoclonal or oligoclonal in origin, indicating that intimal proliferation plays an important role in the development of lesions. Benditt (1973). Intimal proliferation also occurs as a common response to arterial injury of many kinds, regardless of whether the injury is luminal or adventitial. Schwartz (1995). Thus, models of vessel injury  
10       are relevant to atherosclerosis. For example, in a cuff model of adventitial injury, Booth *et al.* (1989); Kockx *et al.* (1993), signals from the adventitia stimulate formation of a neointimal layer in a predictable manner. This model leaves the endothelium intact, so that the role of endothelial gene products can be studied. In a filament model of endothelial injury, Lindner (1993), the endothelium is  
15       physically removed, resulting in proliferation of medial smooth muscle cells. The rate at which endothelial cells resurface the injured areas can be quantitated.

          In another type of atherosclerosis model, defined genetic mutations are used to increase the propensity of mice to atherosclerosis. Breslow (1996); Ross (1996). For example, mutant mice that form atherosclerotic lesions include apoE  
20       gene knockout mice, Plumb (1992); Zhang (1992); apoE Leiden mutation, van der Maagdenberg (1993); LDL receptor gene knockout mice, Ishibayashi (1993); and transgenic mice expressing the human apoB gene, Purcell-Huynh (1995). Of these, apoE knockout mice are an attractive atherosclerosis model, since they develop lesions on a low cholesterol, low-fat diet, and do not require the addition  
25       of cholic acid. These knockout mice develop fatty streaks that progress to fibrous plaques at branchpoints of major vessels, similar to human lesions. The rate and extent of lesion formation and its pathological severity can be quantitated. For example, a Western diet results in faster progression of the disease and formation of larger plaques than a low-cholesterol diet. Thus, the apoE knockout mice  
30       exhibit many aspects of human atherosclerosis.



Nitric oxide has physiological effects in blood vessels that may prevent atherosclerosis, such as suppression of smooth muscle proliferation, Mooradian (1995), inhibition of platelet aggregation and adhesion, Radomski (1991), and inhibition of leukocyte activation and adhesion, Bath (1993); Lefer (1993). It has also been recently reported that arginine inhibits atherosclerosis in LDL receptor mutant mice. Aji (1997).

While certain physiological effects of nitric oxide may prevent atherosclerosis, other studies suggest that excessive nitric oxide production may contribute to the development of atherosclerosis. Busse (1976); Leitinger (1995); Radomski (1995). Evidence for a pro-atherogenic role for nitric oxide includes several different findings. First, expression of iNOS and nNOS isoforms can be induced in atherosclerotic vessels. Aji (1997); Sobey (1995); Topors (1995); Wilcox (1994). Second, human atherosclerotic lesions contain nitrotyrosine, suggesting that peroxynitrite is formed in atherosclerotic lesions. See Beckman (1994b). Peroxynitrite is formed by the reaction of nitric oxide with superoxide in biological systems, Beckman (1994a), and is an extremely potent oxidant that can initiate lipid peroxidation of human LDL. Darley-Usmar (1992). Third, nitric oxide affects redox-sensitive transcription of genes involved in endothelial cell activation such as VCAM-1. This implicates nitric oxide in atherosclerosis.

However, prior to this invention, it was not clear which NOS isoforms were involved in stimulating atherosclerosis. Malinski (1993). Moreover, it was also not clear how important is peroxynitrite formation to the molecular events of atherosclerosis. Peroxynitrite ( $\text{ONOO}^-$ ) is a strong oxidant capable of lipid and protein oxidation. Beckman (1994a). Superoxide reacts with nitric oxide to form peroxynitrite faster, rate constant of  $6.7 \times 10^9$  M/sec, than superoxide is scavenged by superoxide dismutase, rate constant of  $2.0 \times 10^9$  M/sec. Endothelial cells are sensitive to the redox state and may respond with a program of endothelial cell activation, including expression of VCAM-1, ICAM-1, E-selectin, and MCP-1.

Many studies depend on pharmacological agents that block NOS enzymes, such as L-nitroarginine (L-NA) and L-N-arginine methyl ester (L-NAME). Inhibition of a process by these NOS inhibitors, and reversal of inhibition by excess L-arginine, but not D-arginine, provides evidence for the involvement of NO. However, these NOS inhibitors affect all three isoforms, so that the effect on different isoforms cannot be distinguished. Distinguishing between various NOS isoforms is particularly important since NOS isoforms have multiple roles and divergent effects.

Targeted gene disruption of the endothelial or neuronal NOS isoforms offers a new approach to dissect the relevance of NO in brain ischemia and the development of treatments for brain ischemia and stroke. For example, mice deficient in neuronal NOS gene expression were relatively resistant to brain injury after permanent focal cerebral ischemia. Huang *et al.* (1994).

Over the last several years, transgenic animals have been made containing specific genetic defects, e.g., resulting in the development of, or predisposition to, various disease states. These transgenic animals can be useful in characterizing the effect of such a defect on the organism as a whole, and developing pharmacological treatments for these defects.

The relevant techniques whereby foreign DNA sequences can be introduced into the mammalian germ line have been developed in mice. See *Manipulating the Mouse Embryo* (Hogan *et al.*, eds., 2d ed., Cold Spring Harbor Press, 1994) (ISBN 0-87969-384-3). At present, one route of introducing foreign DNA into a germ line entails the direct microinjection of a few hundred linear DNA molecules into a pronucleus of a fertilized one-cell egg. Microinjected eggs may then subsequently be transferred into the oviducts of pseudo-pregnant foster mothers and allowed to develop. It has been reported by Brinster *et al.* (1985), that about 25% of the mice that develop inherit one or more copies of the micro-injected DNA.

In addition to transgenic mice, other transgenic animals have been made. For example, transgenic domestic livestock have also been made, such as pigs, sheep, and cattle.

5 Once integrated into the germ line, the foreign DNA may be expressed in the tissue of choice at high levels to produce a functional protein. The resulting animal exhibits the desired phenotypic property resulting from the production of the functional protein.

10 In light of the various biological functions of nitric oxide, there exists a need in the art to develop transgenic animals, e.g., transgenic mice, wherein the endothelial nitric oxide synthase gene has been modified. There also exists a need in the art to develop methods to test compounds for activity against various pathological states associated with the absence of eNOS, such as hypertension, atherosclerosis, and stroke, using these transgenic animals. A further need in the art is to develop treatments for various pathological states using nitric oxide or  
15 nitric oxide prodrugs.

### *Summary of the Invention*

This invention satisfies these needs in the art by providing a transgenic non-human animal comprising a disrupted endothelial nitric oxide synthase gene. In embodiments of this invention, the transgenic non-human animal exhibits  
20 hypertension or wound-healing abnormalities. In a specific embodiment of the invention, the transgenic non-human animal is a mouse. Moreover, in specific embodiments of this invention, the endothelial nitric oxide synthase gene is disrupted at exons encoding the NADPH ribose and adenine binding sites.

25 In other embodiments, this invention provides a method of testing compounds for activity against a vascular endothelial disorder by providing a transgenic non-human animal having a disrupted endothelial nitric oxide synthase gene, wherein the animal exhibits either a vascular endothelial disorder or is at increased risk of developing the vascular endothelial disorder, administering a

compound to be tested to the transgenic animal, and determining the effect of the compound on the vascular endothelial disorder in the animal. In specific embodiments of this invention, the vascular endothelial disorder is hypertension or atherosclerosis.

5           This invention also provides a method for treating vascular endothelial disorders comprising: selectively increasing the expression of eNOS in blood vessels without increasing the expression of iNOS or nNOS. In specific embodiments, gene therapy approaches are used.

10           In a further embodiment, this invention provides a method of testing compounds for wound-healing activity by providing a transgenic non-human animal having a disrupted endothelial nitric oxide synthase gene, administering a compound to be tested to the transgenic animal, and determining the effect of the compound on the wound-healing capabilities of the animal.

15           In another embodiment, this invention provides a method of treating wounds by applying nitric oxide or a prodrug thereof. In a specific embodiment thereof, compounds which release nitric oxide into wounds to improve or speed up wound healing.

20           In an additional embodiment, this invention provides a method of making a transgenic non-human animal of the invention comprising providing an embryonic stem cell comprising an intact eNOS gene; providing a targeting vector capable of disrupting said eNOS gene upon homologous recombination; introducing said targeting vector into said cells under conditions where the intact eNOS gene of said cell and said targeting vector undergo homologous recombination to produce a disrupted eNOS gene; introducing said cells into a  
25           blastocyst; implanting the blastocyst into the uterus of a pseudopregnant female; and delivering transgenic animals of the invention from said pseudopregnant female. In order to obtain homozygous mutant mice of the invention, the resulting animals can be bred, and homozygous mutant mice selected.

30           In another embodiment, this invention provides a method of testing compounds for utility in the treatment of cerebral ischemia or stroke by providing

a transgenic non-human animal having a disrupted endothelial nitric oxide synthase gene, administering a compound to be tested to the transgenic animal, determining the effect of the compound on infarct size or regional cerebral blood flow (rCBF) following induction of focal cerebral ischemia in the brain of said animal, and correlating the effect of said compound on infarct size or rCBF with a utility for the treatment of cerebral ischemia or stroke. In a preferred embodiment, the eNOS mutant animal has been rendered normotensive.

In a further embodiment, the invention also provides a method for testing compounds for utility in the treatment of atherosclerosis by providing a transgenic non-human animal having a disrupted endothelial nitric oxide synthase gene, administering a compound to be tested for atherosclerosis activity to the transgenic animal, determining the effect of the compound on atherosclerosis, and correlating the effect of said compound on atherosclerosis with a utility for the treatment of atherosclerosis. In specific embodiments, the effect of the compound on atherosclerosis is determined using the vessel or the cuff vessel injury model.

### ***Brief Description of the Figures***

Figure 1 depicts the targeted disruption of the endothelial NOS gene. This Figure shows restriction maps of the native mouse endothelial NOS gene, the targeting vector, and the disrupted eNOS gene. The targeted vector contains 5' and 3' flanking regions of homology and it is designed to replace the *HindIII-SalI* fragment of the eNOS gene containing exons encoding the NADPH ribose and adenine binding sites (amino acids 1010-1144). NEO refers to the neomycin antibiotic resistance gene. The location of the KS probe, used for Southern blot analysis, is also shown.

Figure 2 shows the results of a Southern blot analysis of genomic DNA isolated from mutant mouse tails, digested with *SpeI* and hybridized to the KS probe, shown in Figure 1. Lanes 1, 2, and 3 show wild-type, heterozygous, and homozygous eNOS mutant mice, respectively. The positions of fragments

hybridizing to the wild-type and the disrupted eNOS gene, as depicted in Figure 1, are indicated.

Figure 3 depicts a Western blot analysis of eNOS mutant mice. Brain, heart, lung and aorta samples of wild-type (wt) and mutant (m) mice were tested for immunological reactivity against a mouse monoclonal antibody directed against eNOS. The position of eNOS is shown.

Figure 4 depicts the endothelium-dependent relaxation of aortic rings in response to acetylcholine. Panel a shows the effect on wild-type aortic segments. Panel b depicts treatment of wild-type vessel rings with L-nitroarginine (L-NA), a NOS inhibitor. Panel c depicts the endothelium-dependent relaxation of eNOS mutant aortic segments.

Figure 5 depicts blood pressure responses to L-NA. Urethane-anesthetized wild-type (solid line) and eNOS mutant mice (dotted line) were measured before and after L-NA administration at time 0.

Figure 6 depicts wound healing in eNOS mutant mice. Figure 6A is a micrograph of a 24 hr. wound in a wild-type mouse. Figure 6B is a micrograph of a 5 day wound in a wild-type mouse. Figure 6C is a 24 hr. wound of an eNOS mutant mouse. Figure 6D is a 5 day wound of an eNOS mutant mouse. (ep) refers to the epidermis, while (d) refers to the dermis. Capillaries are indicated by (cap).

Figure 7 depicts infarct size in wild-type and eNOS mutant mice. In Figure 7A infarct volumes were measured in SV-129 mice (A), C57 Black/6 mice (B), eNOS mutant mice without hydralazine treatment (C), and eNOS mutant mice following hydralazine treatment (D). Infarct size was detected 24 hrs after permanent filament MCA occlusion by TTC staining. A statistically significant increase ( $p < 0.05$ ) in infarct size was noted for eNOS mutant animals. Each dot represents the value from an individual animal, and data are expressed as mean  $\pm$  SD.

Figure 7B depicts infarct areas in five coronal sections from rostral to caudal (2 to 10 mm) of the above groups. Open circles, filled circles, and

triangles represent wild-type SV-129 mice, wild-type C57 Black 6 mice, and eNOS mutant mice, respectively. Data shown are means  $\pm$  SD. \* indicates  $p < 0.05$  as compared to both wild-type SV-129 and wild-type C57 Black/6 mice. # indicates  $p < 0.05$  as compared to SV-129 mice alone.

5           Figure 8 depicts regional cerebral blood flow (rCBF) as measured by laser Doppler flowmetry after MCA occlusion in the periinfarct area of eNOS mutant mice (dotted line,  $n=11$ ) as compared to wild-type SV-129 animals (continuous line,  $n=10$ ,  $p < 0.05$ ). A greater rCBF reduction was noted in eNOS mutant mice as compared to wild-type mice. A flexible optic probe tip (diameter = 0.5 mm)  
10       was secured 2 mm posterior and 3 mm lateral to bregma on the ipsilateral hemisphere. Steady-state rCBF values prior to occlusion were taken as a baseline (100%) and the subsequent changes after the onset of ischemia were shown as a percentage relative to baseline. Time zero represents the point of MCA occlusion. There were no significant differences in rCBF blood flow between  
15       SV-129 and C57 Black/6 wild-type mice.

          Figure 9 depicts the effect of hemorrhagic hypotension on rCBF in urethane-anesthetized (dotted line) and wild-type animals (continuous line). Hypotension was induced by gradually withdrawing arterial blood as described *infra*, and rCBF was measured by laser Doppler flowmetry. The initial rCBF  
20       values were taken as 100% and the corresponding changes thereafter calculated as percentage relative to the initial value. The baseline MABF in wild-type and mutants were  $104 \pm 12$  ( $n=7$ ) and  $117 \pm 13$  mm Hg ( $n=7$ ), respectively. There was a greater tendency toward hypoperfusion at higher levels of MABP in the mutant animals. Data are expressed as mean  $\pm$  SD. \* signifies  $p < 0.05$  as  
25       compared to wild-type animals.

          Figure 10 shows that the diameter of pial arterioles was increased in eNOS mutant mice (circle,  $n=7$ ), but not in wild-type (square,  $n=8$ ) mice after nitro-L-arginine superfusion in a closed cranial window. Nitro-L-arginine (1 mM) was topically superfused for 40 minutes. Superfusion of nitro-D-arginine  
30       (1 mM,  $n=3$ ) did not affect the diameter of pial arterioles in eNOS mutant mice

(data not shown). The data are calculated as percent from baseline and expressed as mean  $\pm$  SD. \* indicates  $p < 0.05$  and \*\* indicates  $p < 0.01$  vs. wild-type.

Figure 11 depicts the autoradiographic distribution of [ $^3$ H]L-NA binding in sagittal brain sections of wild-type and mutant mice. Figure 11A is the distribution in SV-129 wild-type mice. Figure 11B is the distribution in C57 Black/6 wild-type mice. Figure 11C is the distribution in eNOS mutant mice. Figure 11D is the distribution in nNOS mutant mice. In Figures 11A-D, OB: olfactory bulb; Str: striatum; HP: hippocampus; DG: dentate gyrus; AM: amygdala; CB: cerebellum. Scale bar=300  $\mu$ m.

Figure 12 depicts the autoradiographic distribution of [ $^3$ H]L-NA binding in coronal sections of SV-129 wild-type mouse brain. Figures 12A -G show total binding. Figure 12H shows binding remaining in the presence of 10  $\mu$ M L-NA. In Figure 12, OB: olfactory bulb; TT: tenia tecta; Str: striatum; RF: rhinal fissure; HP: hippocampus; DG: dentate gyrus; MAN: medial amygdaloid nuclei; CAN: anterior cortical amygdaloid nuclei; VMH: ventromedial hypothalamic nuclei; PC: posteromedial cortical amygdaloid nuclei; PT: piriform transition; LM: lateral mammillary nucleus; SG: superficial grey layer superior colliculus; CB: cerebellum; PR: pontine reticular nucleus. Scale bar=300  $\mu$ m.

Figure 13 depicts the correlation between [ $^3$ H]L-NA binding in mouse and rat brain. 1: granular layer of olfactory bulb, 2: amygdaloid nuclei-posteromedial cortical, 3: amygdaloid piriform transition, 4: amygdaloid nuclei-medial, 5: taenia tecta, 6: rhinal fissure, 7: lateral mammillary nucleus, 8: hippocampal CA3 subfield, 9: amygdaloid nuclei-basomedial, 10: superficial grey layer of superior colliculus, 11: molecular layer of cerebellum, 12: amygdaloid nuclei-anterior cortical, 13: dentate gyrus, 14: amygdaloid nuclei-central, 15: I and II layers of occipital cortex, 16: hippocampal CA1, 17: dorsal tegmental nucleus, 18: plexiform layer of olfactory bulb, 19: I and II layers of frontal cortex, 20: ventromedial hypothalamic nuclei, 21: granule layer of cerebellum, 22: dorsomedial hypothalamic nuclei, 23: medial mammillary nucleus, 24: III to VI layers of occipital cortex, 25: III to VI layers of frontal cortex, 26: striatum, 27:



pontine reticular nucleus, 28: posterior thalamus nuclei, 29: ventral posteromedial thalamus nuclei. Values in mouse and rat brain represent the mean of five SV-129 mice and three rats, respectively.

Figure 14 depicts [ $^3\text{H}$ ]L-NA binding in sagittal sections of SV-129 mouse brain. Figure 14A shows total binding. Figures 14B and 14C, respectively, show binding in the presence of 10  $\mu\text{M}$  D-NA, and 100  $\mu\text{M}$  7-NI, a potent and selective type 1 inhibitor. Figure 14D shows the binding in the presence of excess L-NA (10  $\mu\text{M}$ ). Scale bar=300  $\mu\text{m}$ .

Figure 15 is a schematic showing the effects of nitric oxide produced from various NOS isoforms in normal and atherosclerotic arteries. In Figure 15A, nitric oxide produced by normal endothelium prevents proliferative response to injury and suppresses development of atherosclerosis. In Figure 15B, nitric oxide production in atherosclerotic plaques may lead to peroxynitrite formation, lipid oxidation, and endothelial cell inactivation.

Figure 16 is a schematic showing the cuff model of vessel injury.

Figure 17 depicts micrographs of hematoxylin and eosin stained sections of cuff injured vessels. Injured vessels contain neointima seen inside of the internal elastic lamina (shown with arrows). Control vessels do not contain the neointima. Vessels from eNOS mutant mice show significantly increased neointimal formation, which is shown with an asterisk.

Figure 18 depicts histology and immunochemical staining of injured and control vessels from eNOS mutant mice. Control vessels have no intima.

Figure 19 depicts quantitative RT-PCR of eNOS mRNA from mouse aorta.

Figure 20 depicts atherosclerotic lesions from apoE mutant mice at 6 months. Figure 20A shows the aortic arch and carotid arteries; Figure 20B shows the thoracic aorta; Figure 20C shows the descending thoracic aorta; and Figure 20D shows oil red O stain of an aortic lesion.

### ***Detailed Description of Preferred Embodiments***

5 In the description that follows, a variety of various technical terms are used. Unless the context indicates otherwise, these terms shall have their ordinary well-recognized meaning in the art. In order to provide a clearer and more consistent understanding of the specification and claims, the following definitions are provided.

10 **Transgenic.** As used herein, a "transgenic organism" is an organism containing a defined change to its germ line, wherein the change is not ordinarily found in wild-type organisms. This change can be passed on to the organism's progeny. The change to the organism's germ line can be an insertion, a substitution, or a deletion. Thus, the term "transgenic" encompasses organisms where a gene has been eliminated or disrupted so as to result in the elimination of a phenotype associated with the disrupted gene ("knock-out animals"). The term "transgenic" also encompasses organisms containing modifications to their existing genes and organisms modified to contain exogenous genes introduced into their germ line.

15 **Nitric oxide synthase (NOS).** As used herein, nitric oxide synthase is an enzyme able to catalyze the formation of nitric oxide. For example, NOS can catalyze the formation of nitric oxide from the terminal guanidino nitrogen of arginine, with the stoichiometric production of citrulline.

20 **Disrupted gene.** As used herein, "disrupted gene" refers to a gene containing an insertion, substitution, or deletion resulting in the loss of substantially all of the biological activity associated with the gene. For example, a disrupted NOS gene would be unable to express a protein having substantial NOS enzymatic activity.

25 **Vector.** As used herein, a "vector" is a plasmid, phage, or other DNA sequence, which provides an appropriate nucleic acid environment for a transfer of a gene of interest into a host cell. The cloning vectors of this invention will ordinarily replicate autonomously in eukaryotic hosts. The cloning vector may

be further characterized in terms of endonuclease restriction sites where the vector may be cut in a determinable fashion. The vector may also comprise a marker suitable for use in identifying cells transformed with the cloning vector. For example, markers can be antibiotic resistance genes.

5           **Expression vector.** As used herein, an "expression vector" is a vector comprising a structural gene operably linked to an expression control sequence so that the structural gene can be expressed when the expression vector is transformed into an appropriate host cell.

10           **Targeting vector.** As used herein "a targeting vector" is a vector comprising sequences that can be inserted into a gene to be disrupted, e.g., by homologous recombination. Therefore, a targeting vector may contain sequences homologous to the gene to be disrupted.

This invention relates to non-human transgenic animals comprising a disrupted endothelial NOS gene.

15           In order to obtain a transgenic animal comprising a disrupted eNOS gene, a targeting vector is used. The targeting vector will generally have a 5' flanking region and a 3' flanking region homologous to segments of the eNOS gene surrounding an unrelated DNA sequence to be inserted into the eNOS gene. For example, the unrelated DNA sequence can encode a selectable marker, such as  
20           an antibiotic resistance gene. Specific examples of a suitable selectable marker include the neomycin resistance gene (NEO) and the hygromycin  $\beta$ -phosphotransferase. The 5' flanking region and the 3' flanking region are homologous to regions within the eNOS gene surrounding the portion of the gene to be replaced with the unrelated DNA sequence. DNA comprising the targeting  
25           vector and the native eNOS gene are brought together under conditions where homologous recombination is favored. For example, the targeting vector and native eNOS gene sequence can be used to transform embryonic stem (ES) cells, where they can subsequently undergo homologous recombination. For example,  
30           J1 embryonic stem cells obtained from Dr. En Li of the Cardiovascular Research Center of the Massachusetts General Hospital and Dr. Rudolph Jaenisch of the

Whitehead Institute of MIT. The targeting vector, pPNT-ENOS, has been deposited with the American Type Culture Collection (A.T.C.C.), 12301 Parklawn Drive, Rockville, Maryland 20852 USA, under the terms of the Budapest Treaty under accession number A.T.C.C. 97469 on March 13, 1996.

5 Proper homologous recombination can be tested by Southern blot analysis of restriction endonuclease digested DNA using a probe to a non-disrupted region of the eNOS gene. For example, the KS probe, identified in Figure 1, can be used. Since the native eNOS gene will exhibit a different restriction pattern from the disrupted eNOS gene, the presence of a disrupted eNOS gene can be  
10 determined from the size of the restriction fragments that hybridize to the probe.

In one method of producing the transgenic animals, transformed ES cells containing a disrupted eNOS gene having undergone homologous recombination, are introduced into a normal blastocyst. The blastocyst is then transferred into the uterus of a pseudo-pregnant foster mother. Pseudo-pregnant foster mothers had  
15 been mated with vasectomized males, so that they are in the proper stage of their estrus cycle and their uterus is hormonally primed to accept an embryo. The foster mother delivers a transgenic animal containing a disrupted eNOS gene. Homozygous mutant animals are normally obtained by breeding the transgenic animals.

20 The extent of the contribution of the ES cells, containing the disrupted eNOS gene, to the somatic tissues of the transgenic mouse can be determined visually by choosing strains of mice for the source of the ES cells and blastocyst that have different coat colors.

The resulting homozygous eNOS mutant animals generated by  
25 homologous recombination are viable, fertile, and indistinguishable from wild-type and heterozygous littermates in overall appearance (except for the presence of a selectable marker) or routine behavior. However, the mutant animals can also be sterilized using methods well known in the art, e.g. vasectomy or tubal ligation. See *Manipulating the Mouse Embryo, supra*. The mutant animals can  
30 be mated to obtain homozygous or heterozygous progeny. These mutant animals

contain substantially less immunoreactive eNOS than wild-type animals. Most preferably, these mutant mice contain no immunoreactive eNOS protein as measured by western blot analysis of brain, heart, lung, or aorta tissue.

5 A targeting vector such as pPNT-ENOS can be used to create cell lines or primary cell cultures that do not express NOS. The endogenous eNOS gene can be disrupted by introducing the targeting vector into cells containing the eNOS gene to be disrupted and allowing the targeting vector and the endogenous gene to undergo homologous recombination. For example, the targeting vector can be introduced into the cells by electroporation. If both copies of the eNOS  
10 gene are to be disrupted, higher concentrations of the selection agent, e.g., neomycin or its analog G418 are used. Suitable cell lines and cultures include tumor cells, endothelial cells, epithelial cells, leukocytes, neural cells, glial cells, and muscle cells.

15 The eNOS mutant animals of the invention can be any non-human mammal. In embodiments of this invention, the animal are mice, rats, guinea pigs, rabbits, or dogs. In an especially preferred embodiment of the invention, the eNOS mutant animal is a mouse.

20 These homozygous eNOS mutant animals also exhibit significantly reduced calcium-dependent membrane-associated NOS enzymatic activity. In preferred embodiments of this invention the enzymatic activity in aorta samples is less than  $1.0 \text{ pmol mg}^{-1} \text{ min}^{-1}$   $^3\text{H}$ -arginine to citrulline conversion. In most preferred embodiments of this invention the enzymatic activity in aorta samples is less than  $0.5 \text{ pmol mg}^{-1} \text{ min}^{-1}$   $^3\text{H}$ -arginine to citrulline conversion. Any residual NOS activity may be due to the presence of neuronal NOS (nNOS) in neurons in  
25 the perivascular plexus, and not to the expression of any residual nondisrupted eNOS genes.

Endothelium-derived relaxing factor is absent or significantly reduced in eNOS mutant animals. However, vascular smooth-muscle responses are intact. For example, the aortic rings of mutant mice show no relaxation to acetylcholine,  
30 while aortic rings from wild-type mice manifest a dose-dependent relaxation to

acetylcholine. See Figure 4. Moreover, treatment of wild-type aortic rings with  $10^{-4}$ M L-nitroarginine has no effect on vascular tone by itself, but blocks the relaxation in response to acetylcholine. *Id.* Treatment of the eNOS mutant aortic rings with  $10^{-4}$ M L-nitroarginine also has little or no effect on vessel tone either by itself or on the response to acetylcholine. The maximum dilation of norepinephrine pre-contracted rings from eNOS mutant mice to sodium nitroprusside is similar to wild-type mice. This indicates that vascular smooth-muscle responses in eNOS mutant animals are intact.

The eNOS mutant animals of the invention exhibit various vascular endothelial disorders. These disorders include hypertension and an increased propensity for cerebral ischemia, stroke or atherosclerosis. In addition, the eNOS mutant animals exhibit abnormal wound healing properties. Other vascular endothelial disorders include clotting disorders, other cerebrovascular disorders, coronary artery disease, and peripheral vascular disease. The eNOS mutant animals of the invention exhibit these disorders or an increased propensity of developing these disorders.

Consequently, the eNOS mutant animals are useful as a model to study these and other vascular endothelial disorders. For example, various compounds could be tested for a therapeutic effect on a vascular endothelial disorder by providing a transgenic non-human animal having a disrupted eNOS gene and exhibiting a vascular endothelial disorder; determining the effect of a compound on symptoms of the vascular endothelial disorder; and correlating the effect of the compound on the treatment of the vascular endothelial disorder.

The compounds to be tested are typically not NOS inhibitors. Determining whether a compound exhibits NOS inhibitor activity can be tested based on the information provided herein and in the technical literature. Hevel *et al.* (1994). In preferred embodiments of the invention, compounds that induce NO production are tested; and in more preferred embodiments, compounds that induce NO production in the endothelium are tested. The compounds to be tested can be derived from a variety of sources including, but not limited to, rationally

designed and synthetic molecules, plant extracts, animal extracts, inorganic compounds, mixtures, solutions, and homogeneous molecular or elemental samples.

5 The eNOS mutant animals exhibit a significantly higher blood pressure than the wild-type animals. In specific embodiments of this invention eNOS mutant mice exhibit a mean blood pressure significantly higher than 81 mm Hg. In a preferred embodiment of this invention, eNOS mutant mice exhibit a mean blood pressure greater than about 100 mm Hg. In a most preferred embodiment of this invention, eNOS mutant mice exhibit a mean blood pressure of about 110  
10 mm Hg. Analogous increases in mean blood pressure are expected in other non-murine eNOS mutant (knock-out) animals.

L-NA and other NOS inhibitors cause a rise in blood pressure in many species including humans, rats, guinea pigs, rabbits, dogs, and mice. This effect is consistent with a role of basal nitric oxide production in vasodilation, because  
15 inhibition of eNOS would lead to less basal vasodilation and result in hypertension. However, eNOS mutant mice show a decrease in blood pressure in response to L-NA. See Figure 5. This hypotensive effect is blocked by L-arginine and is not observed with D-nitroarginine. This suggests that pharmacological blockers may have effects in addition to NOS inhibitors, or that  
20 non-endothelial NOS isoforms are involved in the maintenance of blood pressure. For example, nNOS is present both in vasomotor centers of the central nervous system and in perivascular nerves. However, effects of its blockade suggest that it plays a vasodilatory role. Mutant neuronal NOS mice have blood pressures similar to wild-type mice, but they have a tendency towards hypotension when  
25 exposed to anaesthesia, which is consistent with a possible role for nNOS in maintaining, not reducing, blood pressure. Multiple roles for endothelial and non-endothelial NOS isoforms in vasodilation and vasoconstriction may explain the observed variability in maximal pressor effects of various NOS inhibitors.

There is evidence that in hypertension the amount of NO produced by the  
30 endothelium decreases in humans. The eNOS knockout mice mimic this effect,

-22-

since their endothelium also does not produce any NO. Consequently, these mice serve as a useful model for hypertension. Thus, establishing an anti-hypertensive effect in eNOS mutant animals of the invention for a compound other than an NOS inhibitor, such as a compound that induces the production of NO, would be predictive that this compound would have anti-hypertensive properties in other animals, including humans. However, the opposite result would be expected for a compound that inhibits NOS.

An inhibitor of NOS would be expected to raise blood pressure in wild-type animals, but stabilize or reduce blood pressure in eNOS mutant animals. In eNOS mutant animals, an NOS inhibitor would inhibit the residual NOS, mostly nNOS. nNOS mutant animals may have a tendency toward hypotension. Thus, the preferential inhibition of nNOS in the mutant animals should result in the same or lower blood pressure. However, in normal animals, the role of eNOS on blood pressure regulation is much more pronounced than the role of nNOS. Therefore, the predominant effect of an NOS inhibitor in normal animals would be to inhibit eNOS, which raises blood pressure. This is demonstrated in Example 5, *infra*.

In addition, there is also evidence that in atherosclerosis, diabetes and normal aging, the amount of NO produced by the endothelium decreases in humans. Thus, these mice would serve as a useful model not just for hypertension, but also for vascular responses in atherosclerosis, diabetes and normal aging.

The eNOS mutant animals of this invention are useful as an animal model to study hypertension. For example, various compounds could be tested for an anti-hypertensive effect in the eNOS mutant animals. Specifically, compounds that are not NOS inhibitors can be tested. In more preferred embodiments, compounds that are not eNOS inhibitors are tested. In other preferred embodiments compounds that induce NO production are tested. In additional preferred embodiments, compounds that induce NO production in the endothelium are tested. Therefore, the invention provides methods for screening



compounds using the eNOS mutant animals as an animal model to identify compounds useful in treating hypertension. This aspect of the invention is useful to screen compounds from a variety of sources. Examples of compounds that can be screened using the method of the invention include but are not limited to

5 rationally designed and synthetic molecules, plant extracts, animal extracts, inorganic compounds, mixtures, and solutions, as well as homogeneous molecular or elemental samples.

The invention, therefore, provides a method of screening compounds, comprising: providing a transgenic non-human animal having a disrupted eNOS

10 gene and exhibiting hypertension, administering a compound to be tested to the transgenic animal; determining the effect of the compound on the blood pressure of said animal; and correlating the effect of the compound on the blood pressure of the animal with an anti-hypertensive effect of said compound.

The compounds to be tested can be administered to the transgenic non-

15 human animal having a disrupted eNOS gene in a variety of ways well known to one of ordinary skill in the art. For example, the compound can be administered by parenteral injection, such as subcutaneous, intramuscular, or intra-abdominal injection, infusion, ingestion, suppository administration, and skin-patch application. Moreover, the compound can be provided in a pharmaceutically acceptable carrier. *See* Remington's Pharmaceutical Sciences (1990). The effect

20 of the compound on blood pressure can be determined using methods well known to one of ordinary skill in the art.

In addition, the eNOS mutant animals of this invention unexpectedly exhibit abnormal wound-healing properties. For example, these animals often

25 develop spontaneous wounds that do not heal. In contrast to normal mice, who healed their wounds within 5 days, the eNOS mutant mice exhibit significantly different wound healing properties. First, the eNOS mutant mice exhibit spontaneous wounds that never heal. Second, in experiments where wounds were created, the eNOS mutant mice heal more slowly than normal animals. Healing

30 of eNOS mutant mice typically takes 2-3 times as long as normal mice. The

exact healing time will depend on the type of wound inflicted. Moreover, two specific features of normal wound healing are abnormal in the eNOS mutant mice:

- 1) growth of the epithelial layer of skin across the wound to bridge the gap and close the wound; and
- 2) neovascularization in the granulation tissue that fills the wound.

In the eNOS mutant mice, migration of epithelial cells to the site of the wound is delayed, with epithelial cells remaining at the edge of the wound after five days. The connective tissue is also markedly abnormal, containing few or no new blood vessels. The results demonstrate an important role for eNOS in angiogenesis and epithelial cell migration during wound healing.

The eNOS mutant animals of this invention are useful as an animal model to study wound healing. For example, various compounds could be tested for a wound healing effect in the eNOS mutant animals. Therefore, the invention provides methods for screening compounds using the eNOS mutant animals as an animal model to identify compounds useful in enhancing wound healing. This aspect of the invention is useful to screen compounds from a variety of sources. Examples of compounds that can be screened using the method of the invention include but are not limited to rationally designed and synthetic molecules, plant extracts, animal extracts, inorganic compounds, mixtures, and solutions, as well as homogeneous molecular or elemental samples. For example, various compounds designed to improve wound healing can be tested. For example, compounds that deliver NO to the healing wound can be used. Establishing an enhancement of wound healing by a compound in eNOS mutant animals is predictive that this compound would enhance wound healing in other animals, including humans.

The invention, therefore, provides a method of screening compounds, comprising: providing a transgenic non-human animal having a disrupted eNOS gene and exhibiting abnormal wound healing properties, administering a

compound to be tested to the transgenic animal; determining the effect of the compound on the wound healing properties of said animal; and correlating the effect of the compound on the wound healing properties of the animal with a wound healing effect of said compound.

5           Thus, the eNOS mutant animals of this invention are also useful as animal models to study wound healing.

          Moreover, since the synthesis of nitric oxide appears to enhance wound healing, prodrugs that release nitric oxide *in situ* may improve or speed up healing. Examples of suitable compounds that release nitric oxide include  
10   nitroglycerin, sodium nitroprusside, and SIN-1. The extent to which these and other similar compounds improve or speed up wound healing can be determined experimentally. For example, the compound could be applied at the wound to a patient in need of treatment and its effect on wound healing can be quantified.

          The eNOS mutant animals of this invention are also useful as an animal  
15   model to study cerebral ischemia resulting from stroke. Since endothelial NO production may protect brain tissue by increasing ischemic rCBF, compounds can be tested for the ability to increase rCBF as well as the ability to reduce ischemic infarct size. rCBF and infarct size can be measured as described in the Examples. Compounds that increase rCBF or decrease infarct size would be expected to be  
20   useful as therapeutics for the treatment of stroke or cerebral ischemia from other sources.

          It has been reported that nNOS enzymatic activity may contribute to the development of ischemic brain necrosis. In eNOS mutant animals, any non-specific NOS inhibitor would predominantly inhibit the nNOS isoform.  
25   However, in wild-type animals, both eNOS and nNOS would be inhibited. Since eNOS and nNOS have opposite effects under ischemic conditions, with eNOS activity being protective and nNOS activity being detrimental, compounds that are non-specific NOS inhibitors should not be tested for anti-stroke activity. Therefore, in preferred embodiments compounds that are not NOS inhibitors are  
30   tested. In more preferred embodiments, compounds that induce NO production

-26-

can be tested for use as a treatment for stroke or cerebral ischemia. In particularly preferred embodiments, compounds that induce production of NO in the endothelium are tested.

Compounds that can be screened for use in treating stroke or cerebral ischemia can be obtained from a variety of sources. Examples of compounds that can be screened using the method of the invention include but are not limited to rationally designed and synthetic molecules, plant extracts, animal extracts, inorganic compounds, mixtures, and solutions, as well as homogeneous molecular or elemental samples.

The compounds to be tested can be administered to the transgenic non-human animal having a disrupted eNOS gene in a variety of ways well known to one of ordinary skill in the art. For example, the compound can be administered by parenteral injection, such as subcutaneous, intramuscular, or intra-abdominal injection, infusion, ingestion, suppository administration, and skin-patch application. Moreover, the compound can be provided in a pharmaceutically acceptable carrier. *See* Remington's Pharmaceutical Sciences (1990).

The eNOS animals are additionally useful as an animal model to study atherosclerosis. The physiological production of nitric oxide by eNOS suppresses atherosclerosis, whereas the pathologic production of nitric oxide by iNOS and nNOS contributes to atherosclerosis. To test the effect of various compounds on atherosclerosis, various animal models involving eNOS mutant mice are used. Two vessel injury models, the cuff model and the filament model, provide useful data relevant to atherosclerosis. In the cuff model the neointima formation is stimulated by adventitial injury. In the filament model, the endothelium is physically removed, and the rate at which endothelial cells resurface the injured areas is measured. Alternatively, double mutant animals exhibiting aspects of atherosclerosis can be used. For example, double mutant apoE, eNOS mice can be used. Other potential double mutant animals for use in this aspect of the invention include apoE Leiden/eNOS and LDL-receptor eNOS mutants.

By way of example, compounds can be provided to eNOS mutant mice, and the effect of the compound on neointima formation following vessel injury using the cuff model can be determined. The extent of neointima formation can be determined as described in the Examples. Compounds that reduce the extent of neointima formation relative to control eNOS mutant mice not receiving the compound would be expected to be useful as therapeutics for the treatment of atherosclerosis.

In another example, compounds can be provided to eNOS mutant mice and the effect of the compound on the rate at which endothelial cells resurface injured areas of vessels following vessel injury using the filament model can be determined. Compounds that increase the rate of endothelial cell resurfacing relative to control eNOS mutant mice not receiving the compound would be expected to be useful as therapeutics for the treatment of atherosclerosis.

In a further example, compounds can be provided to double mutant animals, which exhibit features of human atherosclerosis. Compounds that reduce symptoms of atherosclerosis in these animals would also be expected to be useful as therapeutics for the treatment of atherosclerosis. A preferred example of a double mutant animal is an apoE/eNOS double mutant.

Since nNOS and iNOS may contribute to atherosclerosis, compounds that are non-specific NOS inhibitors should not be tested for activity against atherosclerosis. Compounds to be tested can be obtained from various sources and administered in various ways as described for other endothelial vascular disorders, *supra*.

Another example of a double mutant animal is eNOS/nNOS mutant mice. These double mutant animals can be obtained by mating eNOS mutant mice to nNOS mutant mice of the same genetic background. Double heterozygous eNOS/nNOS mutant mice are obtained, mating pairs of the double heterozygous mice are obtained, and eNOS/nNOS mutant mice are obtained.

## *Examples*

### *Example 1*

#### *Targeted Disruption of the Endothelial NOS Gene*

5 The endothelial NOS gene was cloned by screening a mouse genomic library, obtained from Stratagene, using a human eNOS cDNA clone, obtained from Kenneth D. Bloch, as described in Janssens *et al.* (1992), Genbank accession number M93718. Plasmid hNOS3C, containing the endothelial nitric oxide synthase gene, was deposited at the American Type Culture Collection on July 17, 1996. The targeting vector was derived from the pPNT vector, which  
10 contains thymidine kinase gene and the neomycin resistance gene. *See* Figure 1. Tybulewicz *et al.* (1991). The targeting vector contains 5' and 3' flanking regions of homology to the eNOS gene, and is designed to replace the *HindIII-SalI* fragment that contains exons encoding the NADPH ribose and adenine binding sites of the eNOS protein (amino acids 1010-1144) following  
15 homologous recombination.

J1 ES cells were grown as described in Li *et al.* (1992) on irradiated embryonic fibroblast feeder cells in media containing 200 units/ml leukocyte inhibitory factor. For electroporation,  $10^7$  cells were mixed with targeting vector DNA at 150  $\mu$ g/ml. A Bio-Rad gene pulsar was used to electroporate the DNA  
20 into the cells at a setting of 960  $\mu$ F capacitance, 250 mV. The targeting vector and the native eNOS gene were then able to undergo homologous recombination. The cells were plated on neomycin-resistant irradiated fibroblast feeder cells, and selection with 150  $\mu$ g/ml G418 and 2  $\mu$ M FIAU was started 48 hours later. Doubly resistant colonies were picked seven days after electroporation and grown  
25 in 24-well plates.

## Example 2

### *Generation of Chimeric Mice with Germline Transmission*

Blastocysts were isolated from C57 BL/6 mice on day 3.5 of pregnancy and 20-25 ES cells, following homologous recombination and selection, were  
5 injected into the uterine horn of pseudo-pregnant (C57 BL/6 x DBA/2) F1 mice. Chimeric mice were identified by the agouti contribution of the ES cells to the coat color, and were back-crossed to C57 BL/6 mice. Germline transmission was determined by the presence of agouti mice in the offspring.

Proper recombination was demonstrated by Southern blot analysis of *SpeI*  
10 digested genomic DNA using the KS probe shown in Figure 1. Back-crossed mice were screened by Southern blot, and heterologous mice were selected. In Figure 1, lanes 1, 2 and 3 show wild-type, heterozygous, and homozygous mutant mice, respectively. The positions of the hybridizing fragments for the wild-type and the disrupted eNOS gene are shown. The results demonstrate that the  
15 targeted disruption of the eNOS gene is present in the germline of the transgenic mice.

Western blot analysis of tissue samples from eNOS mutant mice was also performed. 10  $\mu$ g protein extracts from the brain, heart, lung, and aorta/vena cava of wild-type and eNOS mutant animals were electrophoresed through a 10%  
20 SDS-polyacrylamide gel and transferred to nitrocellulose. The blot was incubated with mouse monoclonal antibodies directed against endothelial NOS (Transduction Research Laboratories), and specific hybridization was localized using chemiluminescent alkaline phosphatase conjugated with anti-mouse antibody (ECL, Amersham). Hybridization of endothelial NOS is observed for  
25 the wild-type samples, but not in the eNOS mutant samples. The heart, lung, and aorta samples show a band at relative molecular mass of 50 kDa in both wild-type and eNOS mutant samples, which represents mouse immunoglobulin heavy chains present in the tissue samples. The antibody used was directed against a

peptide corresponding to amino acids 1030-1209, a region which overlaps with the region deleted in the eNOS mutant mice. See Figure 3. This demonstrates that the eNOS mutant mice (homozygous) produce no immunoreactive undisrupted eNOS, further demonstrating successful transmission of the disruption to the germline of the transgenic mice.

Aorta samples from eNOS mutant mice were tested for calcium-dependent membrane-associated NOS enzymatic activity. This enzymatic activity was reduced to about  $0.5 \text{ pmol mg}^{-1} \text{ min}^{-1}$ . The residual activity is likely due to neuronal NOS in neurons in the perivascular plexus.

### *Example 3*

#### *Determination of blood pressure of eNOS mutant and wild-type mice*

Mice were kept at normal temperature ( $37^{\circ}\text{C}$ ), anesthetized with urethane ( $1.5 \text{ mg/kg}$ , intraperitoneal injection) or halothane inhalation, and ventilated using an SAR-830 mouse ventilator (CWE Instruments). Depth of anesthesia was adjusted to keep the blood pressure of animals unresponsive to tail-pinch with forceps. End-tidal  $\text{CO}_2$  was monitored with a microcapnometer and kept constant by adjustment of respiratory parameters. The right femoral artery was cannulated using stretched PE-10 polyethylene tubing (Clay Adams) for mean arterial blood pressure recordings using an ETH-400 transducer and a MacLab data acquisition system (ADI Instruments). For awake measurements, the femoral artery catheter was placed under halothane anesthesia and the wound was covered with 1% xylocane ointment to diminish discomfort. Recordings were made within one hour of the procedure. Data are expressed as means with standard deviation. Statistical evaluation was performed by t-test.



Table 1. Blood pressure of eNOS mutant and wild-type mice

	Wild-type mice			eNOS mutant mice		
	Urethane	Halothane	Awake	Urethane	Halothane	Awake
Mean BP (mmHG)	81	90	97	110*	109*	117*
s.d.	9	12	8	8	11	10
n	16	15	14	17	18	17

\*P<0.01 for eNOS mutant animals vs. wild-type mice.

There is no statistically significant difference between the blood pressure of nNOS mutant mice and wild-type mice using this procedure.

Similar results are obtained with different methods of anesthesia and in the awake state. Blood pressure is the same for the wild-type SV129 strain, wild-type C57 B16 strain, and litter mates of the eNOS mutant animals that are wild-type at the eNOS locus.

#### Example 4

##### *Endothelium-dependent Relaxation of Aortic Rings in Response to Acetylcholine from eNOS Mutant and Wild-type Mice*

The thoracic aorta was dissected from wild-type and eNOS mutant mice and placed in physiological saline aerated with 95% O<sub>2</sub>/5% CO<sub>2</sub>. 4 mm segments of the aorta were mounted on tungsten wires in conventional myographs and maintained at optimal tension in physiological saline for 1 hour at 37°C. The rings were pre-contracted with 10<sup>-7</sup> M norepinephrine and exposed to increasing concentrations of acetylcholine (ACh) from 10<sup>-8</sup> M to 3 x 10<sup>-5</sup> M. 2-3 segments were collected from each mouse, and five mice were used from the wild-type and eNOS mutant groups. Mean data from each animal were used. Respective tracings are shown. Acetylcholine concentrations are expressed in logM.

Figure 4A depicts wild-type aortic segments responding to acetylcholine with dose-dependent relaxation. At  $3 \times 10^{-5}$  M,  $60.3 \pm 14.6\%$  of pre-addition tone was present. Figure 4B depicts treatment of the wild-type vessel rings with  $10^{-4}$  M L-NA for 1 hour and shows abolished acetylcholine-induced relaxation. Figure 4C shows that eNOS mutant aortic segments do not relax to acetylcholine, demonstrating that EDRF activity is absent from eNOS mutant mice. L-NA has no additional affect on eNOS vessel segments.

Thus, aortic rings from wild-type mice manifest a dose-dependent relaxation to acetylcholine, while aortic rings from eNOS mutant animals show no relaxation to acetylcholine. Treatment of wild-type aortic rings with  $10^{-4}$  M L-NA has no effect on vascular tone by itself, but blocks the relaxation in response to acetylcholine. Treatment of the eNOS mutant aortic rings with  $10^{-4}$  M L-NA has no effect on vessel tone, either by itself or in response to acetylcholine. The maximum dilation of norepinephrine pre-contracted rings from eNOS mutant mice to sodium nitroprusside is no different from wild-type mice, indicating that vascular smooth-muscle responses are intact.

### *Example 5*

#### *Blood Pressure Responses to L-NA for Wild-type and eNOS Mutant Mice*

Mean arterial blood pressure (MABP) of urethane-anesthetized wild-type (solid line in Figure 5) and eNOS mutant mice (dotted line in Figure 5) were measured by femoral artery catheterization and recorded for 30 minutes of baseline before L-NA administration (arrows in Figure 5). At time 0, 12 mg/kg of L-NA was given intraperitoneally. Monitoring for 1 hour shows that the blood pressure of wild-type mice rose from a baseline of 78 mm Hg to 109 mm Hg ( $n = 11$ ). The blood pressure of eNOS mutant mice dropped from a baseline of 98 mm Hg to 66 mm Hg ( $n = 5$ ). Each mouse in the wild-type group responded to L-NA with a rise in blood pressure, and each mouse in the eNOS mutant group

-33-

responded with a drop in pressure. Mean arterial blood pressure differences between wild-type and eNOS mutant animals are statistically significant by the t-test (#,  $p < 0.01$ ). Differences between baseline blood pressures and following L-NA treatment were also statistically significant (\*,  $P < 0.05$  by ANOVA followed by Dunnett). These effects were prevented by L-arginine (200 mg/kg, intraperitoneal), and were not seen with D-nitroarginine (12 mg/kg). The heart rate of eNOS mutant mice and wild-type mice did not differ, and L-NA had no effect on heart rate.

These results support the conclusion that eNOS in the endothelium regulates blood pressure. The major NOS isoform in the endothelium is eNOS. However, a small amount of nNOS is also present. Disruption of the eNOS gene raises blood pressure, while disruption of the nNOS gene stabilizes or lowers blood pressure. Thus, inhibition of NOS in wild-type animals by L-NA, which would predominantly inhibit eNOS, would be expected to raise blood pressure. This is shown in Figure 5. However, inhibition of NOS in eNOS mutant mice would not be expected to raise blood pressure since the effect of L-NA inhibition in the mutants would be to inhibit nNOS and not eNOS. Since nNOS maintains or raises blood pressure levels, *see supra*, inhibition of nNOS would be expected to lower blood pressure levels. This is also seen in Figure 5.

### *Example 6*

#### *Screening of Compounds for Anti-hypertensive Effects using eNOS Mutant Mice*

The eNOS mutant mice exhibit hypertension. Compounds that are associated with NO production in the endothelium, thereby replacing eNOS enzymatic activity, are screened for anti-hypertension activity in eNOS mutant mice. These compounds can be administered to the eNOS mutant mice using pharmaceutically acceptable methods. See Remington's Pharmaceutical Sciences

-34-

(1990). For example, the compound to be screened can be administered at various concentrations by parenteral injection, infusion, ingestion, and other suitable methods in admixture with a pharmaceutically acceptable carrier. The effect of various concentrations of the screened compound on blood pressure is measured relative to control eNOS mutant animals that have not been administered the compound.

A significant decrease in blood pressure of the eNOS mutant mice by a screened compound is indicative that this compound would exhibit beneficial anti-hypertensive properties in other animals and in humans.

### *Example 7*

#### *Wound Healing in eNOS Mutant Mice*

It was observed that eNOS mutant mice, but not wild-type or nNOS mutant mice, tend to develop chronic wounds. Therefore, eNOS mutant mice were tested in a model of wound healing involving a full thickness transverse incision overlying the lumbar area. The incisions penetrated the deep dermis down to the skeletal muscle. In Figure 6, the histological appearance of these wounds at 24 hours and at 5 days following incision, for wild-type and eNOS mutant mice, are shown. At 24 hours, the wounds are very similar. The epidermis (ep) and the deep dermis (d) are transected. Inflammatory cells are seen in both wild-type and eNOS mutant mice.

By five days, wild-type mice have healed. The epithelial layer is reconstituted, and granulation tissue with newly sprouted capillaries fills in the scar. The dermis, which has been cut, remains absent in the healed wound. Thus, normal healing involves two quantifiable features: rapid epithelial migration from the wound edges, and the development of new capillaries, neovasculation, in the connective tissue matrix.

-35-

In these eNOS mutant animals, little or no healing has been observed at 5 days. The migration of epithelial cells is delayed, and the epithelial cells remain at the edge of the wound (ep). The connective tissue is markedly abnormal, and contains few or no new vessels. These results demonstrate an important role for eNOS in angiogenesis and epithelial cell migration during wound healing.

### *Example 8*

#### *Screening of Compounds for Wound Healing Effects using eNOS Mutant Mice*

The eNOS mutant mice exhibit spontaneous wounds. Compounds to be screened for wound healing activity can be administered to the eNOS mutant mice in a pharmaceutically acceptable excipient. For example, the compound can be administered at various concentrations to the wound directly as an ointment or salve. Alternatively, other pharmaceutically acceptable modes of administration can be used. For example, a pharmaceutical composition comprising the compound can be administered by parenteral injection, infusion, ingestion, skin-patch application, and other suitable methods. The effect of the compound is measured relative to control eNOS animals that have not been administered the compound.

A significant enhancement of wound healing on the spontaneous wounds of eNOS mutant mice by a screened compound would indicate that this compound exhibits beneficial wound healing properties in other animals and in humans.

Particularly preferred compounds for screening are compounds known to release NO, such as nitroglycerin, sodium nitroprusside, and SIN-1.

Similarly, eNOS mutant mice having artificially inflicted wounds can also be used in such a screening assay. For example, the effect of various compounds

-36-

on a full thickness transverse incision, as described in the preceding example, can be used as a screening assay.

### ***Example 9***

#### ***Determination of Cerebral Infarct Sizes after Middle Cerebral Artery (MCA) Occlusion in Wild-type and eNOS Mutant Mice***

5

Male and female wild-type (SV-129 and C57 Black/6, Taconic Farms, Germantown, NY) and eNOS mutant mice weighing 20 to 26 g were housed under diurnal lighting conditions and allowed free access to food and water *ad libitum*. Nitro-L-arginine, nitro-D-arginine, hydralazine hydrochloride and 2,3,5-triphenyltetrazolium chloride (TTC) were purchased from Sigma.

10

Mice were anesthetized with 2% halothane for induction and maintained on 1% halothane in 70/30% nitrous oxide/oxygen by mask. The right femoral artery was cannulated with PE-10 polyethylene tubing for arterial blood pressure measurement (Gould, Oxnard, CA) and blood gas determination (Corning 178, Ciba Corning Diag., Medford, MA). Rectal temperature was maintained between 36.5 - 37.5°C with a homeothermic blanket system (YSI, Yellow Springs, OH).

15

Focal cerebral ischemia was induced by occlusion of middle cerebral artery (MCA) using the intraluminal filament technique. Zea-Longa *et al.* (1989); Huang *et al.* (1994). Through a ventral midline incision, the right common and external arteries were isolated and ligated. A microvascular clip (Zen temporary clip, Ohwa Tsusho, Tokyo, Japan) was temporarily placed on the internal artery and the pterygopalatine artery. An 8-0 nylon monofilament (Ethicon, Somerville, NJ) coated with silicone was introduced through a small incision in the common carotid artery and advanced 10 mm distal to the carotid bifurcation so as to occlude the MCA and posterior communicating artery. The wound was sutured and the animal returned to its cage and allowed free access to water and food.

20

25

Twenty-four hours later, animals were sacrificed with an overdoses of pentobarbital and the brains removed and sectioned coronally into five 2-mm slices in a mouse brain matrix. Slices were placed in 2% TTC solution, followed by 10% formalin overnight. Morikawa *et al.* (1994a). The infarction area, outlined in white, was measured (Bioquant IV image analysis system) on the posterior surface of each section, and the infarction volume was calculated by summing the infarct volumes of sequential 2 mm thick sections.

In protocol 1, MCA occlusion was produced in SV-129 (n=12), C57 Black/6 (n=11), eNOS mutant mice (n=14), and eNOS mutant mice injected with hydralazine (1 mg/kg, ip, 1 hr before and 5, 17 hrs after MCA occlusion) to match the arterial blood pressure of wild-type mice (n=10).

In protocol 2, eNOS mutant and wild-type animals were injected with nitro-L-arginine (6 mg/kg, ip, 5 min, 3 and 6 hrs after ischemia) or an equivalent volume of saline vehicle in order to test the hypothesis that inhibition of nNOS activity alleviated ischemic brain injury. The investigator was blinded to the treatment group in this protocol.

As discussed *supra*, the mean arterial blood pressures in eNOS mutant mice were higher ( $115 \pm 8$  mmHg) than wild-type animals ( $98 \pm 7$  mmHg and  $94 \pm 7$  mmHg in SV-129 and C57 B/6, respectively). After hydralazine administration however, mean arterial blood pressures (MABP) did not differ between groups (Table 2).

In this and in Examples 10-11, data are expressed as means  $\pm$  SD. Statistical evaluation was performed by analysis of variance (ANOVA) followed by *t*-test to compare the data among groups in protocol 1. Unpaired Student's *t*-test was used to test the significance between two groups in protocol 2 and rCBF measurement. ANOVA with repeated measures and ANOVA followed by *t*-test were used to evaluate significance within group differences and individual points between groups in the autoregulation experiment. *Probability* values less than 0.05 were considered of statistical significance.

In protocol 1, wild-type SV-129 and C57 Black/6 developed infarcts that were  $37 \pm 7\%$  (n=12) and  $38 \pm 15\%$  (n=11) of their respective hemispheres. Larger infarct volumes ( $46 \pm 9\%$  of hemisphere, n=14,  $p < 0.05$  as compared to wild-type SV-129 and C57 Black/6) were measured in eNOS mutant mice. Larger infarct volumes were also recorded in eNOS mutant mice made normotensive by hydralazine treatment ( $48 \pm 7\%$  of hemisphere, n=10,  $p < 0.05$  vs wild-type SV-129 or C57 Black/6) (Fig. 7A,B). There were no significant group differences in physiology or blood gases before and 24 hrs after MCA occlusion to explain these differences (Table 2).

In protocol 2, administration of nitro-L-arginine decreased infarct volume in the eNOS mutant mice by 24% and injury volumes became equivalent to wild type. Nitro-L-arginine treatment, however, did not change lesion size after MCA occlusion in wild-type mice (Table 3).



Table 2. Physiological data 10 min before MCA occlusion and 24 hrs after ischemia

	pH		pCO <sub>2</sub> (mmHg)		pO <sub>2</sub> (mmHg)		MABP (mmHg)	
	before	after	before	after	before	after	before	after
<b><u>Protocol 1</u></b>								
Wt SV-129	7.33±0.04	7.29±0.06	42.2±4.5	43.8±6.6	153±20	146±29	98±7	95±6
Wt C57 B/6	7.34±0.05	7.35±0.06	49.5±3.1	51.1±4.7	148±30	137±38	94±7	96±4
eNOS mutant <sup>a</sup>	7.33±0.07	7.32±0.08	47.2±4.8	49.6±7.3	139±37	128±35	115±8	117±9
eNOS mutant <sup>b</sup>	7.35±0.04	7.30±0.05	43.8±5.9	47.3±2.9	148±16	139±28	102±6	102±
<b><u>Protocol 2</u></b>								
<b>eNOS mutant</b>								
nitro-L-arginine	7.36±0.07	7.33±0.05	47.6±4.3	51.0±2.9	120±38	134±35	110±10	107±9
Vehicle	7.32±0.07	7.32±0.07	44.6±4.2	43.6±6.3	129±32	138±32	113±8	118±8
<b>Wt SV-129</b>								
nitro-L-arginine	7.36±0.04	7.35±0.03	47.8±3.5	49.3±6.3	142±17	158±22	92±4	97±14
Vehicle	7.37±0.04	7.36±0.03	46.8±4.4	45.6±2.0	134±35	146±28	94±5	98±13

Data are expressed as means  $\pm$  SD. n=5-7 in each group.

<sup>a</sup>: Hypertensive group; <sup>b</sup>: normotensive group treated with hydralazine.

-41-

**Table 3.** Effects of nitro-L-arginine on infarct size 24 hrs after middle cerebral artery occlusion in mice.

	Infarct Volume (mm <sup>3</sup> )	
	Wild-type	eNOS mutant
Vehicle	94 ± 27	116 ± 13
Nitro-L-arginine	97 ± 13	88 ± 23*

Data are expressed as mean ± SD. n=8-12 in each group. \*p<0.05 vs vehicle.

-41-

### ***Example 10***

#### ***Measurement of rCBF in Wild-type and eNOS Mutant Mice Following MCA Occlusion***

In randomly selected mice, rCBF was determined by laser-Doppler flowmetry (Perimed, PF2B, Stockholm, Sweden) and recorded on a MacLab/8 data acquisition system (AD Instruments, Milford, MA). Two fiberoptic probe tips (Perimed PF 319:2, diameter = 0.5 mm) were fixed 2 mm posterior, 3 mm lateral to bregma and 2 mm posterior, 6 mm lateral to bregma on the ipsilateral hemisphere. These two coordinates identify sites on the convex brain surface within the vascular territory supplied by distal and proximal segments of the middle cerebral artery, respectively, and they correspond to peri-infarct zone and deeply ischemic territory, respectively. Yang *et al.* (1994); Huang *et al.* (1994). Steady-state baseline values were recorded before MCA occlusion. rCBF was recorded continuously during and after ischemia and expressed as percentage relative to the baseline value.

As depicted in Figure 8, rCBF reduction was greater in the zone corresponding to the per infarct area ( $30 \pm 16\%$  of baseline,  $n=11$ ), in eNOS mutant mice ( $p < 0.05$ ) as compared to SV-129 ( $40 \pm 13\%$  of baseline,  $n=10$ ), although there was no significant difference in the MCA core territory (data not shown).

#### ***Autoregulation Study***

Mice were anesthetized with urethane (1.5 g/kg, ip) and ventilated (SAR-830 ventilator, CWE Inc., Ardmore, PA) with 70/30% nitrous oxide/oxygen after tracheostomy. Both femoral arteries were cannulated for arterial blood pressure measurement, blood gas determination and for blood withdrawal. Respiratory parameters were adjusted to keep the  $P_aCO_2$  in normal ranges (30-40 mmHg).

The core temperature was kept normothermic as above. The level of rCBF was monitored by laser Doppler flowmetry. Dalkara *et al.* (1995).

Following reflection of the skin and subcutaneous tissue, an rCBF probe tip was secured directly over the parietal skull with glue (Borden Inc, Columbus, OH), away from pial vessels. An initial rCBF recording was taken as 100% and subsequent flow changes were expressed relative to this value. After heparin (10 units, iv) administration, arterial blood pressure was lowered -10 mmHg every 5 min by withdrawing femoral artery blood (0.05-0.15 ml). Corresponding rCBF readings were averaged for each 10 mm Hg stepwise reduction. The duration of total experiment was approximately 2 - 2.5 hrs. The upper limit of autoregulation was not tested in these mice.

When arterial blood pressure was lowered step-wise by controlled hemorrhagic hypotension in wild-type mice, cerebral blood flow stayed relatively constant until <40 mmHg. However, as depicted in Figure 9, at low blood pressures, the autoregulation curve was shifted slightly to the right in eNOS mutant animals, suggesting higher cerebrovascular resistance than wild type at lower perfusion pressures.

The data in Examples 9-10 demonstrate that deletion of the mouse eNOS gene is associated with larger brain infarcts and more pronounced rCBF reductions in corresponding brain regions after MCA occlusion. *See* Figure 8. eNOS mutants also exhibit proportionally lower rCBFs at reduced perfusion pressures during controlled hemorrhagic hypotension. *See* Figure 9. While the reduction in rCBF at reduced perfusion pressure may be due to hypertension in the eNOS mutant animal, no hypertensive changes were noted in the vessel wall or heart on preliminary histopathological analyses. The contribution of high blood pressure to infarct enlargement in eNOS animals was probably minor since infarct size did not change in eNOS mutants made normotensive by hydralazine administration.

Nitro-L-arginine decreased infarct volumes in eNOS mutant mice but not in wild-type animals. Since nNOS is the only constitutively expressed isoform

in eNOS mutant mice, this decrease was likely caused by nNOS inhibition. However, the reductions after nitro-L-arginine treatment were not as large as expected (24% decrease) based on the observation in nNOS mutant, suggesting that either the degree of nNOS inhibition was small using the employed protocol or that undocumented factors such as systemic hypotension induced by nitro-L-arginine, may have attenuated an even greater reduction in infarct size.

### *Example 11*

#### *Increase in Blood Vessel Diameter after Nitro-L-arginine Superfusion in Wild-type and eNOS Mutant Mice*

The mouse head was fixed in a stereotaxic frame and the skull exposed by a longitudinal skin incision. A stainless steel cranial window ring (8.0 mm in inner diameter, 2.0 mm in height) containing three ports was imbedded into a loop of bone wax over the skull. Dental acrylic was then applied. A craniotomy (2 x 1.5 mm) was made in the left parietal bone within the ring of the window. After dura was opened and the brain surface superfused with artificial cerebrospinal fluid (aCSF), a cover glass was placed to close the window. The volume under the window was approximately 0.1 ml. The composition of aCSF was as follows (in mMol/L): Na<sup>+</sup> 156.5, K<sup>+</sup> 2.95, Ca<sup>++</sup> 1.25, Mg<sup>++</sup> 0.67, Cl<sup>-</sup> 138.7, HCO<sub>3</sub><sup>-</sup> 24.6, dextrose 3.7 and urea 0.67. The pH value of aCSF was kept at 7.35-7.45, and monitored continuously with a pH meter (Corning Inc., Corning, NY). The aCSF was superfused by an infusion pump (0.4 ml/min) via a PE-100 tubing connected to a window port. Intracranial pressure was maintained at 5-8 mm Hg. The temperature of aCSF within the windows was maintained at 36.5-37.0°C.

Pial vessels were visualized through a cranial window by an intravital microscope (Leitz, Germany) equipped with a video camera (C2400, Hamamatsu Photonics, Hamamatsu, Japan). The diameter of a single pial arteriole (20-30 µm) was continuously measured by a video width analyzer (C3161, Hamamatsu,

Japan) and recorded using the MacLab data acquisition and analysis system. After baseline stabilization, nitro-L-arginine or nitro-D-arginine solution (1 mM) was superfused into the window and the diameter of pial arteriole measured continuously 40 min thereafter.

5           As depicted in Figure 10, unlike wild-type mice, nitro-L-arginine superfusion alone increased vessel diameter in eNOS mutant animals, reaching maximum at 30 min ( $p < 0.05$  vs wild-type). Similar changes in rCBF were recorded in preliminary experiments by laser Doppler flowmetry using the closed cranial window technique (data not shown). There was no change in MABP  
10           during nitro-L-arginine superfusion. No change was found in pial diameter after nitro-D-arginine superfusion in eNOS mutant mice (data not shown).

          In the eNOS mutant, nitro-L-arginine superfusion inhibits nNOS within subjacent brain parenchyma, and there is published evidence for a contribution from parenchymally-derived NO to cerebrovascular tone. Iadecola *et al.*, 1994.  
15           This example provides evidence that nitro-L-arginine may directly decrease tone in resistance vessels or surrounding tissues of eNOS mutants by showing that nitro-L-arginine superfusion dilates pial arterioles in these mutants. However, the mechanism remains unknown.

          NO is a potent vasodilator and it, or a closely related chemical, is  
20           proposed as EDRF or endothelium-derived relaxing factor. Ignarro *et al.* (1987); Palmer *et al.* (1988). This is evidence to support the hypothesis that endothelium-derived NO or reaction product may be beneficial to stroke by augmenting rCBF in ischemic territory. Infusion of L-arginine, a substrate for NOS, caused NO-dependent vasodilation and increased rCBF distal to MCA occlusion in rats.  
25           Morikawa *et al.* (1994a). Dynamic susceptibility contrast magnetic resonance imaging also suggests that L-arginine infusion cerebral blood flow and blood volume. Hamberg *et al.* (1993). Zhang *et al.* (1994) reported that NO donors improved rCBF in the ischemic area and reduced infarct size as well. In addition, sectioning of NOS-containing parasympathetic cerebrovascular fibers in  
30           sphenopalatine ganglia, Nozaki *et al.* (1993), increased infarct size after focal

ischemia, Kano *et al.* (1991), and reduced cerebral perfusion during hemorrhagic hypotension. Koketsu *et al.* (1992). The above evidence coupled with our observation that arterial blood pressures are less stable in eNOS mutant animals, e.g., during hypercapnic challenge, shows the importance of eNOS regulation of vascular hemodynamics and its potential importance to stroke outcome.

eNOS mutant mice maybe more susceptible to ischemic injury because NO modulates the microcirculation. NO may also block leukocyte adhesion and decrease microvascular stasis often seen following MCA occlusion. Garcia *et al.* (1993). Kubes *et al.* (1991) reported that superfusing mesenteric vessels with NOS inhibitors increased leukocyte adhesion. Kurose *et al.* (1994) found that L-arginine attenuated ischemia-induced platelet-leukocyte aggregation, mast cell degranulation and albumin extravasation. We also found that rCBF was more severely reduced in homologous brain areas after MCA occlusion in eNOS but not nNOS mutant mice. Huang *et al.* (1994). These findings confirm that NO plays a role in the modulation of the microcirculation which may contribute to the outcome of ischemia.

eNOS inhibition may account for the increases in infarct size in some studies after nitro-L-arginine, particularly after large doses. Yamamoto *et al.* (1992); Zhang and Iadecola (1993); Morikawa *et al.* (1994b). By contrast, neuroprotection was reported after selective nNOS inhibition with 7-nitroindazole, Yoshida *et al.* (1994), or FPL17477, Zhang *et al.* (1995). Consistent with present findings, infarction size increased when nitro-L-arginine was administered to mutant mice expressing only the eNOS isoform (i.e., nNOS knockout mouse). Importantly, iNOS enzyme activity is not measurable in mouse (SV-129 strain) brain for at least 4 days after permanent MCA occlusion. Yoshida *et al.* (1995).

We conclude that NO possesses a dual role in focal cerebral ischemia. Depending upon its source, NO may be toxic or protective to brain under ischemic conditions. Parenchymal NO overproduction may lead to neurotoxicity whereas endothelial NO may protect brain tissue by increasing rCBF or some



other hemodynamic mechanism. These results emphasize the importance of knockout mice to dissect the role of individual proteins in these pathophysiological events.

## ***Example 12***

### 5                    ***Brain Distribution of NOS in Wild-type and Mutant Mice***

#### ***Experimental Procedures***

##### ***Animals***

Adult male wild-type, SV-129 and C57black/6 (Taconic Farms, Germantown, NY, U.S.A.), and adult male and female nNOS mutant, Huang *et*  
10 *al.*, *Cell* 75:1273-1286 (1993), and eNOS mutant mice weighing 22 to 29 g and adult male Wistar rats (Charles River, MA, U.S.A.) weighing 250 to 300 g were allowed free access to food and water.

##### ***Tissue preparation***

Mice and rats were sacrificed by decapitation under 2% halothane  
15 anesthesia (30% O<sub>2</sub> + 70% N<sub>2</sub>O). The brains were rapidly removed, immediately frozen in powdered dry ice, and stored at -70°C. Twelve µm sagittal or coronal sections were cut in a cryostat-microtome at -18°C (Leitz 1720, Leica, Deerfield, IL, U.S.A.) and thaw-mounted onto gelatin-coated slides (1% gelatin and 0.1% KCr<sub>2</sub>O<sub>7</sub>). Adjacent sections were stained with cresyl violet and hematoxylin  
20 eosin, and stored at -70°C.

##### ***[<sup>3</sup>H]L-NG-Nitro-arginine autoradiographic binding assay***

The method for the autoradiographic visualization of NOS binding using [<sup>3</sup>H]L-NG-Nitro-arginine ([<sup>3</sup>H]L-NA) has been described previously. Rutherford

*et al.*, (1995). Prior to experiments, sections were brought to -20°C and then to room temperature. Sections were preincubated for 15 min at room temperature in 50 mM Tris-HCl (pH 7.3) to remove the endogenous ligands and/or modulators, then incubated for 30 min at room temperature in 50 mM Tris-HCl buffer containing 10 µM CaCl<sub>2</sub> and 25 nM N<sup>G</sup>-nitro-L-[2,3,4,5-<sup>3</sup>H]arginine hydrochloride ([<sup>3</sup>H]L-NA, specific activity: 48-57 Ci/mmol, Amersham, Arlington Heights, IL, U.S.A.). Unlabelled L-N<sup>G</sup>-nitro-arginine (L-NA, Sigma, St. Louis, MO, U.S.A.), D-N<sup>G</sup>-nitro-arginine (D-NA, RBI, Natick, MA, U.S.A.) and 7-nitroindazole (7-NI, Cookson Chemicals Ltd., England) was added at concentrations of 10, 10, and 100 µM, respectively. The sections were then washed twice for 5 min in ice-cold buffer and rinsed for 10 sec in ice-cold distilled water to eliminate residual buffer. After drying with cold air, the slides were tightly apposed to <sup>3</sup>H-Hyperfilm (Amersham) together with tritiated polymer standards (Amersham) and exposed at -4°C for 6 weeks.

#### *Densitometric analysis*

Films were developed in Kodak D-19 and fixed in Kodak Rapid Fixer, according to the manufacturer's instructions. The optical density of the regions of interest was measured by a computer-assisted image analysis (System M4, Imaging Research, St. Catharines, Ontario, Canada). The relationship between optical density and radioactivity was examined with reference to the tritium standards (Amersham, [<sup>3</sup>H]microscale) co-exposed with the tissue sections. The optical density of the brain regions measured in the present study was in a range in which the optical density and the radioactivity of the <sup>3</sup>H-microscale showed a near linear relationship. The densities of NOS binding sites are expressed in fmol bound [<sup>3</sup>H]L-NA/mg tissue using the [<sup>3</sup>H]L-NA concentration of 25 nM.

### *NOS catalytic activity*

NOS activity was measured by the conversion of [<sup>3</sup>H]arginine to [<sup>3</sup>H]citrulline according to the method described by Bredt *et al.* (1990b) with minor modifications. Samples were homogenized in 500 µl cold 50 mM HEPES buffer (Research Organics Inc., OH, U.S.A.) containing 1 mM EDTA (pH 7.4, Sigma). Homogenates were centrifuged at 500 x g for 5 min. at 4°C and the supernatant used for assay. The incubation mixture contained 100 µl HEPES (50 mM, pH 7.4), EDTA (1 mM), reduced β-nicotinamide adenine dinucleotide phosphate (β-NADPH, 1 mM, Sigma), dithiothreitol (1 mM, Sigma), calmodulin (10 µg/ml, Calbiochem, CA, U.S.A.) and CaCl<sub>2</sub> (1 mM) and 25 µl of 100 mM L-[<sup>3</sup>H]arginine (1 mCi, Dupont NEN, MA, U.S.A.). The reaction was started by adding the supernatant (25 µl) and stopped after 20 min incubation at 37°C by adding HEPES buffer (20 mM, pH 5.5) containing EDTA (2 mM), pH 5.5. The mixture was then applied to cation-exchange columns containing Dowex AG50WX-8 (Na<sup>+</sup> form; Bio-Rad, Richmond, VA, U.S.A.) and eluted with 2 ml of distilled water. [<sup>3</sup>H]Citrulline was measured within eluates by a scintillation spectrometry (Packbeta 1209, LKB, Gaithersburg, MD, U.S.A.).

### *Statistical analysis*

Data are presented as mean ± SE. Statistical comparisons were made by one-way ANOVA and Tukey's multiple-range test or Student's *t*-test using the software super ANOVA (Abacus Concepts, Berkeley, CA, U.S.A.).

### *Results*

#### *Regional distribution of [<sup>3</sup>H]L-N<sup>G</sup>-nitro-arginine binding in the 4 mouse strains (Figs. 11-13, Table 4)*

[<sup>3</sup>H]L-NA binding was heterogeneously distributed in wild-type (SV-129 and C57Black/6) mouse brain, with highest densities (>90 fmol/mg tissue) associated with the granular layer of the olfactory bulb, the medial amygdaloid nuclei, posteromedial cortical amygdaloid nuclei and amygdaloid piriform

transition. Also, the islands of Calleja, tenia tecta, rhinal fissure, hippocampal CA3 subfield, dentate gyrus, anterior cortical and basomedial amygdaloid nuclei, lateral mammillary nucleus, superficial grey layer of the superior colliculus and cerebellar molecular layer contained high densities of [<sup>3</sup>H]L-NA (50-90 fmol/mg tissue). Other area of prominent binding (30-50 fmol/mg tissue) were the plexiform layer of the olfactory bulb, cortical layers I-II, hippocampal CA1 subfield, dorsomedial and ventromedial hypothalamic nuclei, central amygdaloid nuclei and granule layer of cerebellum. The striatum and pontine reticular nucleus showed relatively poor binding (<20 fmol/mg tissue) (Figs 11A, 11B and 12, Table 4). Binding was not significantly different from background in cortical layers III-VI, posterior and ventral posteromedial thalamus nuclei and medial mammillary nucleus (Figs 11A, 11B and 12).

The density of [<sup>3</sup>H]L-NA binding in nNOS mutant mice was significantly decreased in all regions (Fig. 11D). [<sup>3</sup>H]L-NA in eNOS mutant mice was similar to wild-type mice (Fig. 11C, Table 4).

The distribution of [<sup>3</sup>H]L-NA binding was similar in mouse and rat brain as shown in Fig. 13. Although the binding was relatively higher in mouse brain.

***Effects of 7-NI on [<sup>3</sup>H]L-N<sup>G</sup>-nitro-arginine binding (Fig. 14 and Table 5)***

In the presence of 7-NI (100 μM), [<sup>3</sup>H]L-NA binding was significantly decreased in all regions measured in wild-type (Fig.14) and eNOS mutant mice, but not in nNOS mutant mice. In the presence of 7-NI, the densities of [<sup>3</sup>H]L-NA binding did not show significant differences between wild-type, eNOS mutant and nNOS mutant mice (Table 5).

***Effects of L-NA and D-NA on [<sup>3</sup>H]L-N<sup>G</sup>-nitro-arginine binding (Figs. 11, 14 and Table 6)***

In the presence of L-NA (10 μM), the density of [<sup>3</sup>H]L-NA binding sites was very low in all brain regions of all mouse strains (Figs. 11D, 12H). In the presence of D-NA (10 μM), the density of [<sup>3</sup>H]L-NA binding sites was decreased

by approximately 20 to 30% in SV-129 mice (Figs. 14A, 14B, Table 6). Both L-NA and D-NA decreased slightly the binding to the gelatinized slide itself (Fig. 14C, 14D). Binding in brain of the nNOS mutant mice was not significantly higher than background in any regions (Fig. 11D).

5      ***NOS catalytic activity (Table 7)***

10      The highest NOS catalytic activities in SV-129 mice were found in the cerebellum, thalamus/hypothalamus and cerebral cortex/amygdala. Moderate activities were observed in the brain stem, hippocampus, olfactory bulb and striatum. The activities in eNOS mutant mouse brain were similar to those found in SV-129. In nNOS mutant mice NOS activity was dramatically reduced in all regions investigated. Very low levels of residual NOS catalytic activity were measured in type 1 mutant mice (0-1.7% of SV-129) (Table 7).

***Discussion***

15      In this Example, the distribution and density of [<sup>3</sup>H]L-NA NOS binding sites in the brains of wild-type, eNOS mutant mice, and nNOS mutant mice was examined using quantitative *in vitro* autoradiography. Previous studies showed that [<sup>3</sup>H]L-NA binds specifically and stereospecifically to the nNOS isoform in the rat brain. Kidd *et al.* (1995); Michel *et al.* (1993). Specific binding of [<sup>3</sup>H]L-NA to the endothelium of placental blood vessels was recently established by Rutherford *et al.* (1996) using *in vitro* autoradiography. Using similar techniques, we recently observed specific [<sup>3</sup>H]L-NA binding to pig aortic endothelium, which is displaceable by unlabelled L-NA. Hence, this ligand can detect the presence of both eNOS and nNOS by *in vitro* autoradiography.

20      The highest density of [<sup>3</sup>H]L-NA binding was observed in the olfactory bulb, the amygdaloid complex, the islands of Calleja, and the cerebellum (Fig. 12). In general, these regions exhibit the highest NADPH-diaphorase activity and brain NOS positive immunostaining in the mouse, Huang *et al.* (1993), and in the rat, Schmidt *et al.* (1992); Vincent *et al.* (1992). Thus, the density and

distribution of [ $^3\text{H}$ ]L-NA binding presumably reflects the density and distribution of nNOS, the predominant isoform in brain which comprises more than 95% of NOS activity in the brain.

While the density and distribution of binding was similar in the two wild-type strains, it was relatively higher in mouse than rat brain (Fig. 13). In particular, higher binding was detected in the hippocampus of the mouse which may correspond to the greater NADPH-diaphorase activity reported in mouse CA1 pyramidal cells. Wallace *et al.* (1992). Because activity of the inducible isoform, type 2 NOS (iNOS), is undetectable in normal mouse brain, Yoshida *et al.* (1995), it is unlikely to be a major source for [ $^3\text{H}$ ]L-NA binding in our studies. The values of [ $^3\text{H}$ ]L-NA binding in our rat study were higher than those of Kidd *et al.* (1995), although the rank order of binding activity in rat brain regions was similar in both studies. *Id.* These discrepancies may be due to strain differences or different concentrations of added [ $^3\text{H}$ ]L-NA.

[ $^3\text{H}$ ]L-NA binding in nNOS mutant mice was remarkably lower than wild-type or eNOS mutant mice and the L-NA displaceable [ $^3\text{H}$ ]L-NA binding was distributed diffusely throughout the brain (Table 4). Thus, it is presumed that the loss of [ $^3\text{H}$ ]L-NA binding reflected the absence of nNOS. The residual binding probably did not reflect the labeling of eNOS, since the binding in nNOS mutant brain was not stereoselective and could be displaced by both L- and D-NA.

D-NA displaceable binding, detectable in brain of both wild-type strains, may represent an additional binding site for L-arginine unrelated to NOS protein. The fact that both L-NA and D-NA were able to decrease [ $^3\text{H}$ ]L-NA binding to the gelatinized glass slide (see Fig. 14) suggests that the D-NA-displaceable component of [ $^3\text{H}$ ]L-NA binding is non-specific. Therefore, "specific" binding should not be equated with "displaceable" binding, especially when the displacer is the unlabelled tracer, or closely related to the tracer.

Michel *et al.* (1993) reported that L-NA and D-NA displaced [ $^3\text{H}$ ]L-NA binding with  $\text{pI}_{50}$  values, i.e., the logarithm of the concentration of competing compound causing 50% inhibition of [ $^3\text{H}$ ]L-NA binding, of 7.1 and 3.1 (log

molar concentration), respectively. Hence 10  $\mu$ M D-NA is unlikely to affect the [ $^3$ H]L-NA labelling of specific NOS binding sites and could be used to mask part of the non-specific component of [ $^3$ H]L-NA binding.

There was no significant difference between [ $^3$ H]L-NA binding in eNOS mutant and wild-type mice (Fig. 11, Table 4). Furthermore, NOS enzymatic activity in eNOS mutant mice was almost the same as that in wild-type mice (Table 7). Therefore, these results indicate that the expression of eNOS is low in the mouse brain. However, Dinerman *et al.* (1994) reported the presence of eNOS in the hippocampal pyramidal cells, the cerebellum and olfactory bulb by immunohistochemistry in the rat brain. This discrepancy may reflect species differences and/or the technical differences between quantitative autoradiography and immunohistochemistry.

[ $^3$ H]L-NA binding was inhibited by 7-NI in wild-type and eNOS mutant mice, but not in nNOS mutant mice (Table 5). Hence, the results indicate that binding site of 7-NI in the mouse brain is mainly to nNOS. 7-NI and related substituted indazoles are potent and competitive nNOS inhibitors, Babbedge *et al.* (1993); Moore *et al.* (1993a); Moore *et al.* (1993b), and have been useful for treatment of focal ischemia damage *in vivo*, Yoshida *et al.* (1994), MPTP neurotoxicity *in vivo*, Schulz *et al.* (1995a) and NMDA-induced excitotoxicity *in vivo*, Schulz *et al.* (1995b). 7-NI may also compete with L-arginine for binding to the prosthetic heme group, and affect the pteridine site of the enzyme. Mayer *et al.* (1994). The mechanism of selective nNOS inhibition remains unclear. However, 7-NI at 10 mg/kg i.p., decreases NOS catalytic activity by approximately 30 to 40% within the mouse cerebellum, cerebral cortex and hippocampus. Moore *et al.* (1993); Moore *et al.* (1993). 7-NI does not increase blood pressure, like other NOS inhibitors. Babbedge *et al.* (1993). Moreover, the similarity in [ $^3$ H]L-NA binding in eNOS mutant mice and wild-type mice further supports the use of eNOS mutant mice to screen compounds for use in the treatment or prevention of cerebral ischemia or stroke.

***Conclusion***

This regional distribution of [<sup>3</sup>H]L-NA binding was similar to that seen with the NADPH-diaphorase method. The density of [<sup>3</sup>H]L-NA binding in nNOS mutant mice was dramatically reduced in all regions, compared with wild-type mice, but not eNOS mutant mice. nNOS in mouse brain may represent the majority of [<sup>3</sup>H]L-NA binding sites. [<sup>3</sup>H]L-NA autoradiography may provide a useful method for estimating the distribution of NOS, effects of drugs and pathogenesis of NO-related diseases such as stroke, Alzheimer's disease and tumor. For example, it should be useful for estimating regional changes in NOS binding after cerebral ischemia.



**Table 4.** Regional distribution of L-NA displaceable ( $^3\text{H}$ )L-N<sup>G</sup>-nitro-arginine binding in wild-type (SV-129 and C57black/6) and mutant (eNOS and nNOS mutant) mice.

	Brain regions	Wild-type		Mutant	
		SV-129	C57black/6	eNOS	nNOS
5	Olfactory bulb-granular layer	106 ± 2.5	101 ± 12.1	108 ± 3.8	13 ± 1.6 <sup>*,#</sup>
	Olfactory bulb-plexiform layer	43 ± 3.1	32 ± 3.1	33 ± 1.6	18 ± 0.6 <sup>*,#</sup>
	Islands of Calleja	71 ± 7.9	70 ± 13.7	51 ± 3.5	5 ± 0.6 <sup>*,#</sup>
	Tenia tecta	85 ± 6.7	106 ± 8.0	94 ± 6.1	13 ± 0.6 <sup>*,#</sup>
	Rhinal fissure	84 ± 5.2	80 ± 5.8	70 ± 3.9	17 ± 2.0 <sup>*,#</sup>
10	Striatum	18 ± 1.4	16 ± 1.7	12 ± 0.7	9 ± 0.7 <sup>*,#</sup>
	Frontal cortex I-II	40 ± 1.4	40 ± 3.0	32 ± 2.6	19 ± 1.5 <sup>*,#</sup>
	Occipital cortex I-II	47 ± 4.6	42 ± 5.9	36 ± 3.9	16 ± 0.9 <sup>*,#</sup>
	Hippocampal CA1 subfield	44 ± 2.4	42 ± 5.1	43 ± 2.3	13 ± 1.3 <sup>*,#</sup>
	Hippocampal CA3 subfield	70 ± 2.5	63 ± 4.0	63 ± 2.2	13 ± 1.1 <sup>*,#</sup>
15	Dentate gyrus	57 ± 4.6	56 ± 4.0	52 ± 1.1	14 ± 1.2 <sup>*,#</sup>
	Dorsomedial hypothalamic nuclei	34 ± 2.6	25 ± 4.2	29 ± 6.0	12 ± 1.4 <sup>*</sup>
	Ventromedial hypothalamic nuclei	42 ± 5.8	47 ± 7.4	45 ± 5.9	13 ± 1.8 <sup>*,#</sup>
	Amygdaloid complex				
	Amygdaloid nuclei-medial	90 ± 5.6	96 ± 8.8	89 ± 4.2	14 ± 2.2 <sup>*,#</sup>
20	Amygdaloid nuclei-anterior cortical	57 ± 7.9	73 ± 8.6	69 ± 5.7	15 ± 2.9 <sup>*,#</sup>
	Amygdaloid nuclei-basomedial	70 ± 5.7	53 ± 7.7	63 ± 8.2	13 ± 1.9 <sup>*,#</sup>
	Amygdaloid nuclei-central	48 ± 6.5	41 ± 2.4	33 ± 4.4	14 ± 2.1 <sup>*,#</sup>
	Amygdaloid nuclei-posteromedial cortical				
	Amygdaloid piriform transition	101 ± 5.0	98 ± 5.7	98 ± 3.5	15 ± 1.5 <sup>*,#</sup>
25	Lateral mammillary nucleus	91 ± 6.3	93 ± 5.9	87 ± 5.1	13 ± 0.7 <sup>*,#</sup>
	Superficial grey layer superior colliculus	71 ± 6.3	52 ± 5.4	52 ± 3.7	13 ± 1.6 <sup>*,#</sup>
	Cerebellum				
	Molecular layer	67 ± 4.4	54 ± 4.4	61 ± 5.4	16 ± 3.3 <sup>*,#</sup>
	Granule layer	64 ± 4.2	70 ± 4.9	67 ± 7.0	14 ± 3.0 <sup>*,#</sup>
30	Pontine reticular nucleus	40 ± 2.2	42 ± 4.6	42 ± 3.6	13 ± 2.7 <sup>*,#</sup>
		14 ± 1.3	10 ± 1.9	10 ± 0.4	6 ± 1.4 <sup>*</sup>

30 Values (fmol/mg tissue) represent mean ± S.E. of five mice per group and were determined by subtracting binding remaining in the presence of 10  $\mu\text{M}$  L-NA from the total binding in serial sections. \*:  $p < 0.01$  vs. SV-129, #:  $p < 0.01$  vs. C57black, +:  $p < 0.01$  vs. type 3 mutant (Turkey's multiple range test).

**Table 5.** Effects of 7-NI on the regional distribution of [<sup>3</sup>H]L-NA binding in wild-type (SV-129 and C57black/6) and mutant (type 3 and type 1) mice.

Brain regions	Wild-type		Mutant	
	SV-129	C57black/6	eNOS	nNOS
Olfactory bulb (granular layer)				
5 L-NA displaceable <sup>1)</sup>	109 ± 1.9	113 ± 9.9	106 <sup>3)</sup>	33 ± 1.9
	7-NI <sup>2)</sup> 17 ± 0.7	28 ± 4.1*	N.T.	30 ± 2.7
Hippocampal CA3 subfield				
10 L-NA displaceable	60 ± 3.1	53 ± 2.3	50 ± 6.2	25 ± 0.9
	7-NI 18 ± 1.8*	22 ± 4.7*	21 ± 1.8*	23 ± 2.3
Dentate gyrus				
10 L-NA displaceable	48 ± 2.6	58 ± 5.6	58 ± 5.4	28 ± 2.2
	7-NI 18 ± 0.7*	22 ± 4.6*	20 ± 2.7*	22 ± 1.7
Amygdaloid complex				
15 L-NA displaceable	90 ± 4.9	89 ± 11.3	88 ± 2.9	29 ± 1.4
	7-NI 21 ± 2.1*	21 ± 4.8*	21 ± 2.9*	23 ± 2.5
Cerebellum (molecular layer)				
L-NA displaceable	67 ± 1.7	78 ± 6.8	67 ± 5.8	30 ± 0.8
	7-NI 18 ± 1.3*	23 ± 5.4*	20 ± 2.2*	24 ± 1.0

Values (fmol/mg tissue) represent mean ± S.E. of three mice per group.

20 <sup>1)</sup>: L-NA displaceable = (total -binding in the presence of 10μM L-NA) binding

<sup>2)</sup>: 7-NI = L-NA displaceable binding in the presence of 100 μM 7-NI,

<sup>3)</sup>: n=1, N.T.: not tested,

\*: p<0.01 vs. L-NA displaceable. There are no significant differences between L-NA displaceable and 7-NI groups in type 1 mice.

**Table 6.** Effects of D-nitro-arginine (D-NA) on the regional distribution of [ $^3$ H]L-NA binding in wild-type (SV-129) and nNOS mutant mice.

Brain Regions	Binding	SV-129	nNOS mutant
Olfactory bulb (granular layer)			
	L-NA displaceable <sup>1)</sup>	121 $\pm$ 12.4	32 $\pm$ 2.3 <sup>#</sup>
	D-NA <sup>2)</sup>	92 $\pm$ 10.8	5 $\pm$ 3.0 <sup>*,#</sup>
Hippocampal CA3 subfield			
	L-NA displaceable	83 $\pm$ 2.4	33 $\pm$ 4.2 <sup>#</sup>
	D-NA	66 $\pm$ 5.9	3 $\pm$ 1.9 <sup>*,#</sup>
Dentate gyrus			
	L-NA displaceable	67 $\pm$ 3.7	33 $\pm$ 5.5 <sup>#</sup>
	D-NA	43 $\pm$ 4.8	2 $\pm$ 1.9 <sup>*,#</sup>
Amygdaloid complex			
	L-NA displaceable	96 $\pm$ 12.6	32 $\pm$ 5.9 <sup>#</sup>
	D-NA	64 $\pm$ 7.6	3 $\pm$ 1.7 <sup>*,#</sup>
Cerebellum (molecular layer)			
	L-NA displaceable	86 $\pm$ 4.5	32 $\pm$ 6.2 <sup>#</sup>
	D-NA	59 $\pm$ 6.7	0 $\pm$ 3.6 <sup>*,#</sup>

10 Values (fmol/mg tissue) represent mean  $\pm$  S.E. of four to five mice per group.

<sup>1)</sup>: L-NA displaceable = (total - binding remaining in the presence of 10  $\mu$ M L-NA) binding;

<sup>2)</sup>: D-NA = L-NA displaceable binding in the presence of 10  $\mu$ M D-NA,

\*: p<0.01 vs. L-NA displaceable, #: p<0.01 vs. SV-129

**Table 7.** NOS catalytic activity in SV-129, eNOS mutant and nNOS mutant mice.

Brain regions	NOS catalytic activity (fmol/mg wet weight/min)		
	SV-129	eNOS mutant	nNOS mutant
Olfactory bulb	3.1 ± 0.9	4.0 ± 1.2	0 ± 0 <sup>#</sup>
Striatum	2.4 ± 0.3	2.4 ± 0.8	0.04 ± 0.04 <sup>*,#</sup>
5 Thalamus/Hypothalamus	6.2 ± 1.8	5.8 ± 1.2	0.07 ± 0.04 <sup>*,#</sup>
Hippocampus	3.1 ± 0.9	3.2 ± 0.5	0.03 ± 0.03 <sup>*,#</sup>
Cerebral cortex/Amygdala	4.0 ± 1.0	4.0 ± 0.7	0.07 ± 0.02 <sup>*,#</sup>
Cerebellum	9.0 ± 2.0	7.3 ± 1.7	0.04 ± 0.04 <sup>*,#</sup>
Brain stem	3.3 ± 0.7	3.5 ± .09	0.05 ± 0.05 <sup>*,#</sup>

- 10 \*: p<0.05 vs. SV-129, #: p<0.05 vs. type 3 mutant mice (Turkey's multiple range test).  
 NOS catalytic activity was measured by calcium-dependent [<sup>3</sup>H]arginine to [<sup>3</sup>H]citrulline conversion. The experiment was performed three times in duplicate.

### *Example 13*

#### *Use of the Vessel Injury Models of Atherosclerosis in eNOS Mutant Mice*

- 15 Both the cuff model and the filament model of vessel injury can be used  
 as an animal model for atherosclerosis. Major features of these two vessel injury  
 models can be seen in the following Table:

**Table 8.** Comparison of Vessel Injury Models

20	Feature	Cuff Model	Filament Model
	Exemplary Location	femoral artery	carotid artery
	Method of Injury	placement of non-occlusive cuff around vessel	insertion of filament to denude endothelial layer
	Manipulated Area	adventitia	endothelium

Response	adventitial inflammation; medial cellular proliferation	removal of endothelium, medial cellular proliferation
Time to response	14-28 days	14-28 days
Measurements	quantitative morphometry; immunohistochemistry; expression studies (RT-PCR); indices of cellular proliferation	quantitative morphometry; immunohistochemistry; expression studies (RT-PCR); indices of cellular proliferation

***The Cuff Model:***

5 Mice aged 7-8 weeks were anesthetized with pentobarbital (50 mg/kg ip). Femoral arteries were surgically exposed and dissected from the surrounding tissue. A nonocclusive polyethylene cuff (2 mm in length, 0.58 mm inner diameter, made of PE-50 tubing split longitudinally) was placed around the left femoral artery and tied snugly with a silk thread. The right femoral artery served  
10 as a sham control. The wounds were then closed and the animals allowed to awaken from anesthesia. Animals were euthanized at 3, 14, 21, and 28 days after cuff placement. The femoral arteries were fixed under perfusion in 10% formalin, and embedded in paraffin.

The cuffed vessel segment and the corresponding sham operated vessel  
15 were cut into 200 serial 10  $\mu$ m sections, and were placed in order on five series of slides, as shown in Figure 16. One series was stained with hematoxylin-eosin, another with elastin, and the others were saved for immunohistochemistry. The slides were scanned into Adobe Photoshop, and the quantitative morphometry was performed using the public domain program *NIH Image*.

20 We performed two types of measurements. First, for area/volume measurements, the areas within the lumen, internal elastic lamina, and external elastic lamina were measured. The intimal area was calculated as the difference between the area within the internal elastic lamina and the lumen. The medial area was calculated as the difference between the areas within the external and

internal elastic laminae. The areas were integrated over the length of the vessel segment to calculate the volume of intima and media. Second, for thickness measurements, the thickness of the intima and the media at four points located 90° to each other, and averages over the length of the vessel segment.

5 Table 9 shows the representative data from individual wild-type and eNOS mutant male mice, to indicate the types of measurements and their variance.

(wild-type male mice)

No.	Genotype	Sex	Age	Wt, g.	Linear measurements, $\mu\text{m}$								
					Volume measurements			Injured side			Control side		
					Intima	Media	I/M ratio	Lum diam	Intima	Media	Lum diam	Intima	Media
70	Wild-type	M	8	24.0	5.9	25.1	0.23	111.4	7.9	27.7	110.9	0	28.8
71	Wild-type	M	8	23.0	7.5	23.1	0.32	210.1	5.5	15.6	166.2	0	23.5
72	Wild-type	M	8	24.0	6.5	22.8	0.28	172.8	5.8	17.9	154.9	0	22.4
73	Wild-type	M	8	25.9	8.9	31.5	0.28	160.4	8.3	23.4	118.7	0	29.8
74	Wild-type	M	8	26.1	5.4	23.6	0.23	198.5	4.9	17.1	211.6	0	20.0
75	Wild-type	M	8	24.3	6.7	24.5	0.27	227.3	3.2	15.6	162.6	0	27.3
76	Wild-type	M	8	23.9	9.3	32.7	0.28	212.5	6.8	21.1	153.8	0	20.3
77	Wild-type	M	8	25.0	6.3	26.9	0.23	142.7	6.7	23.1	183.7	0	25.8
78	Wild-type	M	8	23.0	10.7	39.5	0.27	172.5	9.3	28.6	159.2	0	32.5
79	Wild-type	M	8	26.3	10.9	41.8	0.26	198.1	6.1	21.4	183.3	0	27.6
132	Wild-type	M	8	26.1	11.3	35.6	0.32	182.4	6.5	18.7	176.6	0	26.9
133	Wild-type	M	8	25.2	8.1	32.8	0.25	142.7	6.7	29.9	183.7	0	30.8
134	Wild-type	M	8	23.8	10.7	39.5	0.27	172.5	9.3	28.6	159.2	0	31.9
135	Wild-type	M	8	25.9	8.7	25.9	0.33	150.6	8.3	24.5	180.3	0	22.3
136	Wild-type	M	8	24.8	7.6	26.4	0.29	162.6	5.1	26.8	156.1	0	18.6
137	Wild-type	M	8	22.9	11.2	31.2	0.36	180.0	5.9	21.6	180.1	0	20.7
138	Wild-type	M	8	26.8	7.5	28.6	0.26	195.2	6.3	19.6	196.5	0	23.9
139	Wild-type	M	8	26.3	10.2	29.2	0.35	186.3	7.0	25.4	198.5	0	22.6
140	Wild-type	M	8	25.9	9.1	29.8	0.30	210.1	4.9	28.0	168.2	0	23.6
141	Wild-type	M	8	22.9	8.5	23.6	0.36	175.4	8.6	24.8	145.3	0	29.0
Mean					8.5	29.7	0.29	178.2	6.6	22.9	167.5	0	25.4
Std. dev.					1.9	5.8	0.04	28.3	1.6	4.5	24.7	0	4.2

(eNOS mutant male mice)

No.	Genotype	Sex	Age	Wt, g.	Linear measurements, $\mu\text{m}$								
					Volume measurements			Injured side			Control side		
					Intima	Media	I/M ratio	Lum diam	Intima	Media	Lum diam	Intima	Media
98	eNOS -/-	M	8	28.0	20.8	32.1	0.65	122.5	22.8	26.3	116.4	0	27.7
99	eNOS -/-	M	8	25.2	23.5	36.6	0.64	165.5	20.1	25.3	131.9	0	27.3
100	eNOS -/-	M	8	23.5	33.2	36.4	0.91	203.6	29.4	20.5	133.3	0	25.7
101	eNOS -/-	M	8	20.5	19.7	27.9	0.71	136.9	20.0	22.3	151.3	0	31.1
102	eNOS -/-	M	8	22.7	22.5	33.4	0.67	144.9	21.5	25.0	138.1	0	33.6
103	eNOS -/-	M	8	25.8	21.5	30.6	0.70	157.4	21.5	23.9	134.1	0	30.5
104	eNOS -/-	M	8	23.6	19.8	31.2	0.63	146.6	19.0	23.8	168.4	0	29.6
105	eNOS -/-	M	8	28.1	21.4	36.0	0.59	177.6	15.2	24.6	159.4	0	28.1
106	eNOS -/-	M	8	21.0	16.3	23.4	0.70	157.6	13.2	19.3	162.7	0	26.3
147	eNOS -/-	M	8	26.6	21.7	30.5	0.71	160.2	20.3	23.4	181.2	0	24.5
148	eNOS -/-	M	8	25.8	23.1	36.2	0.64	180.9	24.1	24.3	167.4	0	22.8
149	eNOS -/-	M	8	24.2	26.2	29.9	0.88	149.2	25.9	23.8	162.4	0	23.1
150	eNOS -/-	M	8	20.6	25.2	31.5	0.80	150.2	24.6	23.1	155.2	0	23.8
151	eNOS -/-	M	8	26.6	27.0	34.3	0.79	150.9	28.9	23.8	153.7	0	24.6
152	eNOS -/-	M	8	28.4	22.2	32.2	0.69	188.6	19.2	24.6	180.4	0	24.8
153	eNOS -/-	M	8	27.5	26.5	26.8	0.99	139.5	23.5	24.1	138.5	0	28.3
154	eNOS -/-	M	8	29.7	21.7	29.1	0.75	154.2	18.8	22.5	168.0	0	21.6
155	eNOS -/-	M	8	25.4	23.3	31.1	0.75	132.0	22.5	23.1	151.8	0	25.4
156	eNOS -/-	M	8	24.3	24.6	32.6	0.75	168.5	26.5	21.3	160.2	0	22.5
157	eNOS -/-	M	8	24.0	21.3	30.3	0.70	156.4	16.7	22.5	165.3	0	27.0
Mean					23.1	31.6	0.73	157.2	21.7	23.4	154.0	0.00	26.4
Std. dev.					3.5	3.4	0.10	19.6	4.2	1.7	17.2	0.00	3.2

These results are summarized in Table 10. Wild-type mice, which have no detectable intima at baseline, develop neointima within 14 days of cuff injury, with an intima to media (I/M) volume ratio of 0.29 for males and 0.18 for females. The eNOS mutant animals developed substantially more neointima, with an I/M volume ratio of 0.73 for males and 0.43 for females. Thus, animals with a disrupted eNOS gene exhibit greater neointimal formation in response to cuff injury. Figure 17 shows representative section of vessels stained with hematoxylin-eosin. The internal elastic lamina is indicated by arrows, and the degree of neointima formation can be easily seen.

**Table 10. Neointima Formation Measured 14 Days After Cuff Placement**

Mouse strain	Intima volume	Media volume	I/M ratio	Intima ( $\mu\text{m}$ )
Wild-type, males (n=20)	0.0085 $\pm$ 0.0019	0.0297 $\pm$ 0.0058	0.29 $\pm$ 0.04	6.6 $\pm$ 1.6
Wild-type, females (n=20)	0.0059 $\pm$ 0.0018	0.0321 $\pm$ 0.0087	0.18 $\pm$ 0.06	4.9 $\pm$ 1.8
eNOS mutant, males (n=20)	0.0231 $\pm$ 0.0035	0.0316 $\pm$ 0.0034	0.73 $\pm$ 0.10	21.7 $\pm$ 4.2
eNOS mutant, females (n=20)	0.0123 $\pm$ 0.0028	0.0286 $\pm$ 0.0062	0.43 $\pm$ 0.09	11.7 $\pm$ 2.7

In Table 10, all measurements are expressed as mean  $\pm$  standard deviation. Volumes are expressed in  $\text{mm}^3$ , and are calculated as outlined in the text from area measurements. The last column shows thickness measurements of intima on the injured side. There was no detectable intima on the control side.  $p < 0.05$  was obtained for each gender, eNOS mutant mice vs. wild-type mice by ANOVA followed by Dunnett statistical analysis.

Figure 18 shows the histology and immunochemical staining of the cuff-injured and control vessels from eNOS mutant mice. Hematoxylin-eosin and elastin stains outline the intima clearly on the injured side; the control has no intima. Cells throughout the neointimal layer stain strongly for actin (E). This staining is also seen in the media of injured and control vessels (E, F), consistent

with smooth muscle staining. In contrast, only the luminal cells stain for von Willebrand factor, a marker of endothelial cells, as shown in panels G and H.

***The Filament Model:***

A comparison of the eNOS mutant mice and wild-type mice using the filament model of vessel injury is performed. As a first step, the size of the carotid arteries of eNOS mutant mice, nNOS mutant mice, and wild-type mice have been quantitated. Carotid arteries were fixed by perfusion at a pressure of 100 mm Hg. The luminal diameter was calculated by dividing the luminal circumference by  $\pi$  to account for differences in luminal shape. As shown in Table 11, the diameters of the carotid artery of wild-type mice do not differ substantially from those of the NOS mutant mice (n=20 in each group). Thus, the filament model can be used with a comparable degree of injury between different mouse strains.

**Table 11.** Luminal diameters of perfusions fixed carotid arteries

	Wild-type	eNOS mutant	nNOS mutant
Mean (mm)	0.42	0.45	0.41
Std. dev. (mm)	0.06	0.08	0.05

The filament model addresses eNOS expression by non-endothelial cells, since it removes the endothelial layer of cells. The filament injury model is performed in eNOS mutant mice and C57BL/6 wild-type mice, and morphometry, immunohistochemistry, and BrdU staining is performed as outlined. Briefly, the external carotid artery is identified, and two ligatures are placed around it. The artery is tied distally and a filament is inserted through an incision and advanced down the common carotid artery. The filament is rotated and passed three times. The external carotid artery is tied off proximally, and the right carotid artery serves as a sham operated control.



The process of endothelial resurfacing, which occurs by migration from uninjured areas such as the aortic arch, is also studied. It is expected that the rate of resurfacing of the endothelial layer following denudation will be much slower in eNOS mutant mice.

5           In order to examine endothelial regeneration, animals are injected with Evan's blue solution (150  $\mu$ l of 5% solution in PBS, iv) 10 minutes before euthanasia to identify de-endothelialized segments. Vessel segments are cut open longitudinally and pinned onto Teflon cards with the lumen facing up. For determination of smooth muscle cell proliferation, mice are injected  
10 intraperitoneally with 5'-bromo-2'-deoxyuridine (BrdU, 25 mg/kg, Boehringer Mannheim) one hour prior to euthanasia. Immunostaining with antibody to BrdU is carried out.

          This result would demonstrate that eNOS expression in both endothelial and non-endothelial cells affect the response to injury. However, if no  
15 differences between mutant and wild-type mice are observed, these results would suggest that local production of eNOS by the endothelium and not other cells, is the overriding factor determining vessel response to filament injury.

          Two independent methods are used to characterize vessel morphometry: area/volume calculations and thickness measurements of the intima and the  
20 media. Intimal, medial, and luminal volumes are calculated by integrating areas along the injured region to ensure that inhomogeneities in neointimal formation along the length of the injured region do not give spurious results. Absolute volumes and intima/media (I/M) ratios are compared. The I/M ratio is a standardized measure that accounts for differences in vessel size, even within the  
25 same group of animals.

          The effect of hypertension in vascular injury responses (both filament and cuff models) is measured by repeating the experiments after treating eNOS mutant mice with hydralazine to reduce their blood pressure to normotensive levels. The addition of hydralazine to drinking water at 250  $\mu$ g/ml gives a daily  
30 dose of about 750  $\mu$ g, and results in a stable decrease in mean arterial pressure

from 102 mm Hg to 72 mm Hg, which is equivalent to the blood pressure of untreated wild-type C57BL/6 mice. This will control hypertension during the duration of the experiment (3 to 28 days). Alternatively, local gene therapy to express eNOS in the femoral artery of the eNOS mutant mice could be used, leaving systemic eNOS deficiency and hypertension unaltered.

### Example 14

#### *Quantitative RT-PCR to Study Expression of NOS Isoforms*

Primers for RT-PCR detection of NOS isoforms in small amounts of tissue from mice have been devised, and are shown below:

The nNOS (type I) primers are as follows:  
 B1 primer: 5' CCT TAG AGA GTA AGG AAG GGG GCG GG 3' (26-mer)  
 B2 primer: 5' GGG CCG ATC ATT GAC GGC GAG AAT GAT G 3' (28-mer)  
 These primers amplify a 404 bp fragment from nNOS cDNA.

The eNOS (type III) NOS primers are as follows:  
 E1 primer: 5' GGG CTC CCT CCT TCC GGC TGC CAC C 3' (25-mer)  
 E2 primer: 5' GGA TCC CTG GAA AAG GCG GTG AGG 3' (24-mer)  
 These primers amplify a 254 bp fragment from eNOS cDNA, and an 800 bp fragment from the eNOS gene.

The iNOS (type II) NOS primers are as follows:  
 I1 primer: 5' ATC AGG AAC CTG AAG CCC CAG GAC 3' (24-mer)  
 I2 primer: 5' TGT TGC CAG ATT TCT CTG CAC GGT 3' (24-mer)  
 These primers amplify a 338 bp fragment from iNOS cDNA.

These primers are specific, and do not prime cDNA corresponding to the other NOS isoforms.

The quantitative nature of this technique was validated by using fixed amounts of aorta RNA (5µg) as starting material for reverse transcription. Vessels are frozen in liquid nitrogen and homogenized in the presence of phenol and guanidine isothiocyanate (RNAzol B). Total cellular RNA is prepared by extraction of the homogenate with chloroform and isopropanol. The proportion of eNOS mutant mRNA to wild-type mRNA varied 100% eNOS mutant (no

wild-type mRNA) to 0% eNOS mutant (100% wild-type RNA). Using these mixtures, first strand cDNA was synthesized and used as a template for PCR using the eNOS specific primers. As seen in Figure 19, the amount of PCR product varied according to the amount of eNOS RNA present in the initial RNA sample, validating the quantitative nature of the reaction. Additional controls for expression of actin and GAPDH were performed as well.

### *Example 15*

#### *ApoE/NOS Mutant Mice*

ApoE mutant mice of a C57BL/6 genetic background were obtained from Jackson Labs. These mice were mated to eNOS mutant mice and nNOS mutant mice of the same genetic background. Double heterozygous apoE/eNOS and apoE/nNOS mice have been obtained. Mating pairs of each double heterozygous mice were bred, and the genotype of the offspring is determined using Southern blot analysis. For example, the ApoE mutation is genotyped by digesting genomic DNA with *HindIII* and using a 0.6 kb *SacI/HindIII* fragment. A ubiquitous endogenous *HindIII* band is 7.5 kb, the wild-type band is about 9 kb, and the disrupted band is 3 kb. See Huang (1994); Huang (1995).

The development of atherosclerotic lesions in the aorta of apoE mutant mice have been observed over time. Figure 20 shows a 6 month old apoE mutant mice with macroscopically visible lesions within the aortic arch, the origins of the carotid arteries, and the thoracic and abdominal aorta. Lipid in an aortic lesion stains with oil red O. The apoE mutant mice develop fatty streak lesions by 10 weeks of age, and evolve foam cells and fibrous plaque lesions by 15-20 weeks. The lesions typically occur in regions of shear stress, at the origins of the carotid arteries, intercostal arteries, renal arteries, and aortic bifurcation.

Since the apoE single or double mutant mice develop predictable, spontaneous atherosclerotic lesions, they provide a genetic background on which to study the effect of mutations in other genes, e.g., eNOS. The development of

atherosclerotic lesions in mice homozygous for apoE and eNOS mutations is compared vs. apoE mutant mice that are wild-type for eNOS.

The animals will be fed a typical high-cholesterol, high-fat Western-type diet to mimic the human atherosclerotic process. This diet contains 16% crude fat, 1.25% cholesterol (Harlan Teklad Diets, Madison, WI). The mice have elevated VLDL and chylomicron levels. The lipid profiles of these mice will also be measured to ensure that eNOS gene disruption does not independently affect the lipid profile.

ApoE and ApoE/eNOS mutant mice are sacrificed at age 5, 10, 20, and 30 weeks. The lungs, liver, stomach, and intestines are removed so that the thoracic and abdominal aorta can be dissected. The tissue is stained with Oil Red O to quantitate the total area of atherosclerotic lesions compared with the area of aorta, from the aortic valve down to 1 cm past the aortic bifurcation. The time points are selected to determine if there is a difference in the rate of lesion development versus the severity of the lesions. The dependence of apoE atherosclerosis on diet demonstrates that these variables can be modulated, and that their quantitation is feasible.

Serial sections are taken for histologic analysis and to quantitate intimal proliferation. The volume of intima is calculated by integrating their affected areas over the length of the affected segment, as described above in the injury models. The cell types involved in these lesions, e.g., smooth muscle, endothelium, and foam cells, are identified by immunohistochemical staining with antibodies for alpha actin, vimentin, factor VIII related antigen, and CD31. The expression of remaining NOS isoforms will be examined by immunocytochemistry, and quantitated by RT-PCR, as described *supra*.

In other experiments, a low-fat, low-cholesterol diet can be used if the effect of the apoE mutation masks the effect of the eNOS mutation. Alternatively, cholic acid can be added to the diet to increase the atherosclerotic stimulus.

-67-

In these experiments, statistical differences in lipid levels among groups are tested by one-way ANOVA, and post hoc tests of individual means are performed with Tukey's test. Differences in atherosclerotic lesion area between groups will be statistically analyzed with the non-parametric Kruskal-Wallis procedure.

### ***Example 16***

#### ***iNOS and nNOS Isoforms Contribute to the Development of Atherosclerosis***

In this Example, iNOS and nNOS mutant mice are used to determine if the loss of these pro-atherogenic isoforms show less response to injury and less atherogenesis. The cuff model of vessel injury is used in iNOS and nNOS mutant mice. These mice have normal vascular anatomy, so their response can be compared with those of wild-type C57BL/6 mice. Quantitative morphometry, immunohistochemistry, indices of cellular proliferation, and NOS isoform studies are performed as part of the filament or cuff injury models as described *supra*.

Double mutant apoE/iNOS and apoE/nNOS mice are bred to compare the development of atherosclerotic lesions in these animals with apoE mice. A typical high-cholesterol, high-fat Western type diet without cholic acid is used to mimic the human atherosclerotic process. The lipid profiles of these animals are measured, to ensure that the disruption of iNOS or nNOS do not have independent effects on the lipid profile.

The mice are sacrificed at age 5, 10, 20, 25, and 30 weeks. The thoracic and abdominal aorta is stained with Oil Red O, to quantitate the total area of atherosclerotic lesions compared with the area of the aorta. Serial sections are taken for histological analysis and to quantitate intimal proliferation. the volume of intima is calculated by integrating the affected areas over the length of the affected segment. The cell types involved in these lesions are identified by immunohistochemical staining, and expression of the remaining NOS isoforms will be examined by immunohistochemistry, and quantitated by RT-PCR.

-68-

This experiment extends the results from injury models to the development of atherosclerotic lesions. The development of lesions involves not only cellular differentiation, but also the recruitment of inflammatory cells, lipid oxidation and phagocytosis, and endothelial cell activation. Due to the participation of iNOS or nNOS isoforms in the pathophysiology of atherosclerosis, the disruption of these genes would be expected to result in a less severe phenotype than apoE mutant mice alone.

### ***Example 17***

#### ***The Effect of NOS Isoform Expression Patterns on Lipid Oxidation and Endothelial Cell Activation***

Peroxynitrite is formed in biological systems only by the reaction of nitric oxide with superoxide. Since human atherosclerotic lesions contain nitrotyrosine, it is known that at least one isoform of NOS generates nitric oxide and peroxynitrite in atherosclerotic lesions. iNOS and nNOS, but not eNOS, are believed to be involved in the generation of peroxynitrite. If so, iNOS and nNOS mutant mice will exhibit decreased amounts of nitrotyrosine. Therefore, atherosclerotic lesions in animals that lack apoE and each isoform (eNOS/apoE, iNOS/apoE, nNOS/apoE) are examined for the presence of nitrotyrosine.

Two independent methods to detect 3-nitrotyrosine are used: immunohistochemical detection and HPLC. For immunohistochemistry, a rabbit antiserum specific for nitrotyrosine, obtainable from Upstate Biotechnology is used. Alternatively, the level of nitrotyrosine is independently assessed by 16 electrode HPLC. Schultz (1996).

Briefly, tissue from a 50  $\mu$ m section of brain, comparable to the amount of tissue in atherosclerotic plaques, is used for this analysis. Atherosclerotic plaques from apoE and apoE/NOS double mutant mice are dissected and frozen. The level of 3-nitrotyrosine will be measured by HPLC with 16 electrode electrochemical detection. Reaction of standards and tissue extracts with 1M

sodium hydrosulfite should abolish the peaks by converting 3-nitrotyrosine to aminotyrosine. The levels of 3-nitrotyrosine are expressed as a ratio of 3-nitrotyrosine to total tyrosine, to normalize for the varying arterial concentrations of tyrosine. This method is more quantitative than immunohistochemical detection and offers an independent measure of nitrotyrosine formation.

Under physiological conditions, eNOS suppresses the expression of endothelial activation genes by inducing and stabilizing I $\kappa$ B. Peng (1995). In atherosclerotic lesions, NOS expression patterns change, and iNOS and/or nNOS expression increases, while eNOS levels drop. Wilcox (1994). These changes are believed to contribute to increased oxidant stress in the vessel wall, and endothelial cell activation. To test for endothelial cell activation, the expression of VCAM-1 can be used as a preferred marker, since its expression is longer lived than other markers. However, ICAM-1, E-selectin and MCP-1 can be used. eNOS mutant mice will exhibit greater expression of VCAM-1 (more endothelial activation) in atherosclerotic lesions, while iNOS and nNOS would be expected to show diminished VCAM-1 expression (less endothelial activation).

VCAM-1 expression is examined by two methods: immunohistochemistry and RT-PCR quantitation of mRNA expression. For immunohistochemistry, a rat monoclonal anti-VCAM-1 antibody obtained from Southern Biotechnology Associates, Inc., Birmingham, AL, is used as the primary antibody, and biotinylated goat anti-rat antibody as a secondary antibody. For RT-PCR primers that amplify VCAM-1 cDNA, conditions are used that ensure that the amount of amplified PCR product is proportional to the level of mRNA. Actin mRNA will be used to standardize the amount of total mRNA, and internal quantitative standards will be employed as described *supra*.

Lipid peroxidation results in many changes, including altered electrophoretic mobility and modification of apolipoprotein B. Many of these can be assessed in purified LDL that has been subject to oxidation, but are more difficult to study *in vivo*. The protein modification epitopes malondialdehyde-

-70-

lysine (MDA-lysine) and 4-hydroxynonenal-lysine (4HNE-lysine) as markers for lipid oxidation events. Palinski *et al.* (1989); Palinski *et al.* (1994); Itabe *et al.* (1994); Yla-Herttuala (1989). These epitopes are found in atherosclerotic lesions in apoE-deficient mice and humans. A panel of antibodies against MDA-lysine and 4-HNE epitopes is used to study whether the absence of any one of the NOS isoforms results in a reduction in staining, implicating that NOS isoform in lipid oxidation. These results are correlated with a histologic assessment of lesion extent, severity, and the presence of foam cells, macrophages, and other inflammatory cells. Independent methods to measure the same process are used, e.g., HPLC for nitrotyrosine or RT-PCR for VCAM-1 expression to improve our ability to detect differences due to NOS isoform deletion.



*Literature Cited*<sup>1</sup>

- Aji *et al.* (1997), *Circulation* 95:430-437.
- Archer, S., (1993), *FASEB J.* 7:349-360.
- Babbedge *et al.* (1993), *Br. J. Pharmacol.* 110:225-228.
- 5 Bath (1993), *Eur. J. Clin. Pharmacol.*, 45:53-58.
- Beckman *et al.* (1994a), *Methods Enzymol.* 233:229-240.
- Beckman *et al.* (1994b), *Biol. Chem. Hoppe-Seyler* 375:81-88.
- Benditt *et al.* (1973), *Proc. Natl. Acad. Sci. (USA)* 70:1753-1756.
- Boeckvstaens *et al.* (1991), *Br. J. Pharmacol.* 102:434-438.
- 10 Bohme *et al.* (1991), *Eur. J. Pharmacol.* 199:379-381.
- Booth *et al.* (1989), *Atherosclerosis* 76:257-268.
- Bredt *et al.* (1994), *Ann Rev. Biochem.* 63:175-195.
- Bredt *et al.* (1992), *Neuron* 8:3-11.
- Bredt *et al.* (1990a), *Nature* 347:768-770.
- 15 Bredt *et al.* (1990b), *Proc. Natl. Acad. Sci. USA.* 87:682-685 (1990) - 129/130
- Breslow (1996), *Science* 272:685-688.
- Brinster *et al.* (1985), *Cell* 27: 4438-4442.
- Bult *et al.* (1990) *Nature* 345: 346-347.
- Burnett *et al.* (1992), *Science* 257: 401-403.
- 20 Busse *et al.* (1996), *J. Vasc. Res.* 33: 181-194.
- Curran *et al.* (1989), *J. Exp. Med.* 170:1769-1774.
- Dalkara *et al.* (1994), *Brain Pathol.* 4:49-57.
- Dalkara *et al.*, (1995), *J Cereb Blood Flow Metab.* 15:631-638.
- Darley-Usmar *et al.* (1992), *Free Rad. Res. Commun.* 17:19-20.
- 25 Dawson *et al.*, (1991) *Proc Natl Acad Sci USA.* 88:6368-6371.
- Dawson *et al.* (1992), *Ann. Neurol.* 32: 297-311.
- Desai *et al.* (1991), *Nature* 351:477-479.
- Dimmeler *et al.* (1992), *J. Biol. Chem.* 267: 16771-16774.
- Dinerman *et al.* (1994), *Proc. Natl. Acad. Sci. (USA)* 91:4214-4218.
- 30 Edelman & Gally (1992), *Proc. Nat'l Acad. Sci. (USA)* 89:11651-11652.
- Furchgott *et al.* (1980), *Nature* 288:373-376.
- Furchgott (1988), Studies on the relaxation of the rabbit aorta by sodium nitrate: basis for the proposal that the acid-activatable component of the inhibitory factor from retractor penis is inorganic nitrate and the endothelium-derived relaxing factor is nitric oxide, In: *Mechanisms of Vasodilation*, P.M. Vanhoutte ed.
- 35 Furchgott & Vanhoutte (1989), *FASEB J.* 3: 2007-2018.
- Gally *et al.* (1990), *Proc. Nat'l Acad. Sci. (USA)* 87:3547-3551.
- Garcia *et al.* (1993), *Am J Pathol.* 142:623-635.

---

<sup>1</sup> All of the literature cited in this application is expressly incorporated herein by reference.

- Gibson *et al.* (1990), *Br. J. Pharmacol.* 99: 602-606.  
Gillespie *et al.* (1989), *Br. J. Pharmacol.* 98: 1080-1082.  
Haley *et al.* (1992), *Neuron* 8: 211-216.  
Hamberg *et al.* (1993) In: *Proceedings of the Society of Magnetic Resonance in Medicine, 12th Annual Scientific Meeting*, Society of Magnetic Resonance in Medicine NY. 1:397.  
Hevel *et al.* (1994), *Methods Enzymol.* 233:250-258 (1994).  
Hibbs *et al.* (1988), *Biochem. Biophys. Res. Comm.* 157: 87-94.  
Huang *et al.* (1993), *Cell* 75:1273-1286.  
Huang *et al.* (1994), *Science* 265:1883-1885.  
Huang *et al.* (1995), *Nature* 377:239-242.  
Iadecola *et al.* (1994), *J Cereb Blood Flow Metab.* 14:175-192.  
Ignarro *et al.* (1988), *Proc. Natl. Acad. Sci. USA.* 84:9265-9269.  
Ignarro (1989), *FASEB J.* 3: 31-36.  
Ishibashi *et al.*, *J. Clin. Invest.* 92: 883-893.  
Itabe *et al.* (1994), *J. Biol. Chem.* 269:15274-15279 (1994).  
Jannsens *et al.* (1992), *J. Biol. Chem.* 267:14519-14522, and erratum published in *J. Biol. Chem.* 267:22694.  
Kano *et al.* (1991), *J Cereb Blood Flow Metab.* 11:628-637.  
Kaufman *et al.* (1995), *Handbook of Molec. and Cell. Methods in Biol. and Medicine*, pp. 329-366.  
Kidd *et al.* (1995), *Neuropharmacol.* 34:63-73.  
Knowles *et al.* (1992), *Trends Biochem Sci.* 17:399-402.  
Kockx *et al.* (1993), *Arterioscl. Thromb.* 13: 1874-1884.  
Koketsu *et al.* (1992), *J Cereb Blood Flow Metab.* 12:613-620.  
Kots *et al.* (1992), *FEBS Lett.* 300: 9-12.  
Kubes *et al.* (1991), *Proc. Natl. Acad. Sci. USA.* 88:4651-4655.  
Kurose *et al.* (1994), *Circ Res.* 74:376-382.  
Lamas *et al.* (1992), *Proc. Natl. Acad. Sci. (USA)* 89:6348-6352.  
Lefer *et al.* (1993), *Arterioscler. Thromb.* 13:1874-1884.  
Leitinger *et al.* (1995), *J. Physiol. Pharmacol.* 46: 385-408.  
Li *et al.* (1992), *Cell* 69: 915-926.  
Linder *et al.* (1993), *Circ. Res.* 73:792-796.  
Lowenstein & Snyder (1992), *Cell* 70: 705-707.  
Malinski *et al.*, *J. Cereb. Blood Flow Metab.* 13: 355-358.  
Marletta (1989), *Trends Biochem. Sci.* 14: 488-492.  
Marletta (1993), *J. Biol. Chem.* 268: 12231-12234.  
Mayer *et al.* (1994), *Neuropharmacol.* 33:1253-1259.  
McDonald & Moss (1993), *Proc. Nat'l Acad. Sci (USA)* 90: 6238-6241.  
Michel *et al.* (1993), *Br. J. Pharmacol.* 109:287-288.  
Moncada (1992), *Acta Physiol. Scand.* 145:201-227.  
Moncada *et al.* (1991), *Pharmacol. Rev.* 43: 109-142.  
Moore *et al.* (1993a), *Br. J. Pharmacol.* 108:296-297.  
Moore *et al.* (1993b), *Br. J. Pharmacol.* 110:219-224.  
Mooradian *et al.* (1995), *J. Cardiovasc. Pharmacol.* 25: 674-678.

- Morikawa *et al.* (1994a), *Stroke*. 25:429-435.  
Morikawa *et al.* (1994b), In: *The human brain circulation (J Bevens, eds.)*, Harbor Basin Conference, Vermont. 373-387.  
Murphy *et al.* (1993), *Trends Neurosci.* 16:323-328.  
5 Nathan (1992), *FASEB J.* 6: 3051-3064.  
Nathan & Xie (1994), *Cell* 278:915-918.  
Nozaki *et al.* (1993), *J. Cereb. Blood Flow Metab.* 13: 70-79.  
O'Dell *et al.* (1991), *Proc. Nat'l Acad. Sci. (USA)* 88: 11285-11289.  
O'Dell *et al.* (1994), *Science*. 265:542-546.  
10 Palinski *et al.*, *Proc. Natl. Acad. Sci (USA)* 86:1372-1376 (1989).  
Palinski *et al.*, *Arterioscler. Thromb.* 14:605-616 (1994).  
Palmer *et al.* (1987), *Nature* 327: 524-526.  
Palmer *et al.* (1988), *Nature*. 333:664-666.  
Peng *et al.* (1995), *J. Biol. Chem.* 270: 14214-14219.  
15 Plump *et al.* (1992), *Cell* 71:343-353.  
Purcell-Huynh *et al.* (1995), *J. Clin. Invest.* 95: 2246-2257.  
Radomski *et al.* (1991), *Trends in Pharm. Sci.* 12:87-88.  
Radomski *et al.* (1995), *Atherosclerosis* 18: S69-80.  
Rajfer *et al.* (1992), *N. Engl. J. Med.* 326: 90-94.  
20 Ramagopal & Leighton (1989), *Eur. J. Pharmacol.* 174: 297-299.  
Ramdomsky *et al.* (1990), *Proc Natl Acad Sci USA.* 87:5193-5197.  
Rees *et al.* (1990), *Br J Pharmacol.* 101: 746-752.  
Remington's Pharmaceutical Sciences, Mack Publishing Co., Easton, PA (1990).  
Ross (1996), *Nature Medicine* 2:527-528.  
25 Ross (1995), *Ann. Rev. Physiol.* 57:791-804.  
Rutherford *et al.* (1995), *Br. J. Pharmacol.* 116:3099-3109.  
Schmidt & Walter (1994), *Cell* 78:919-925.  
Schmidt *et al.* (1992), *J. Histchem. Cytochem.* 40:1439-1456.  
Schultz *et al.* (1996), *J. Neurochem.* 67:430-433.  
30 Schulz *et al.* (1995a), *J. Neurochem.* 64:936-939.  
Schulz *et al.* (1995b), *J. Neurosci.* 15: 8419-8429.  
Schuman & Madison (1991), *Science* 254: 1503-1506.  
Schwartz *et al.* (1995), *Circulation Res.* 77: 445-465.  
Shibuki & Okada (1991), *Nature* 349: 326-328.  
35 Snyder *et al.* (1991), *Trends Pharmacol Sci.* 12:125-128.  
Snyder (1992), *Science* 257: 494-496.  
Snyder (1995), *Nature* 377:196-197.  
Sobey *et al.* (1995), *Circ. Res.* 77: 536-543.  
Toda & Okamura (1990), *Biochem. Biophys. Res. Comm.* 170: 308-313.  
40 Topors *et al.* (1995), *Circulation* 92:I-564.  
Tottrup *et al.* (1991), *Am. J. Physiol.* 260:G385-G387.  
Tybulewicz *et al.* (1991), *Cell* 65: 1153-1163.  
van den Maagdenberg *et al.* (1993), *J. Biol. Chem.* 268: 10540-10545.  
Vincent *et al.* (1992), *Neurosci* 46:755-784.  
45 Wallace *et al.* (1992), *NeuroReport* 3:953-956.

- Wilcox *et al.* (1994), *Circulation* 90 (supp I):I-298.  
Yamamoto *et al.* (1992), *J Cereb Blood Flow Metab.* 12:717-726.  
Yang *et al.* (1994), *Stroke* 25:165-170.  
Yla-Herttuala *et al.*, *J. Clin. Invest.* 84:1086-1095 (1989).  
5 Yoshida *et al.* (1994), *J Cereb Blood Flow Metab.* 14:924-929.  
Yoshida *et al.* (1995), *Neuroscience Letter.* 194:214-218.  
Zea-Longa *et al.* (1989), *Stroke.* 20:84-91.  
Zhang *et al.* (1992), *Science* 258:468-471.  
Zhang *et al.* (1993), *NeuroReport.* 4:559-562.  
10 Zhang *et al.* (1994), *J Cereb Blood Flow Metab.* 14:217-226.  
Zhang *et al.* (1995), *J Cereb Blood Flow Metab.* 15(Suppl.):S90.  
Zhang & Snyder (1992), *Proc. Nat'l Acad. Sci (USA)* 89: 9387-9385.

***What Is Claimed Is:***

1. A method of screening compounds for potential utility to treat cerebral ischemia or stroke, comprising:

5 (a) providing a transgenic non-human animal having a disrupted endothelial nitric oxide synthase gene;

(b) administering a compound to be tested to said transgenic animal;

(c) determining the effect of said compound on infarct size following induction of focal cerebral ischemia in the brain of said animal; and

10 (d) correlating the effect of said compound on infarct size with a potential therapeutic utility to treat cerebral ischemia or stroke;

wherein said compound is not a NOS inhibitor.

2. The method of screening compounds as claimed in claim 1, wherein said transgenic non-human animal is a mouse.

15 3. The method of screening compounds as claimed in claim 1, wherein the blood pressure of said transgenic non-human animal has been rendered normotensive.

4. The method of screening compounds as claimed in claim 2, wherein said compound induces nitric oxide synthesis in the endothelia.

-76-

5. The method of screening compounds as claimed in claim 4, wherein said compound does not induce neuronal nitric oxide overproduction.

6. The method of screening compounds as claimed in claim 4, wherein focal ischemia is induced by occluding the middle cerebral artery.

5 7. A method of screening compounds for potential utility to treat atherosclerosis, comprising:

(a) providing a transgenic non-human animal having a disrupted endothelial nitric oxide synthase gene;

(b) administering a compound to be tested to said transgenic animal;

10 (c) determining the effect of said compound on atherosclerosis in said animal; and

(d) correlating the effect of said compound on atherosclerosis in said animal with a potential utility to treat atherosclerosis;

wherein said compound is not a NOS inhibitor.

15 8. The method of screening compounds as claimed in claim 6, wherein determining the effect of said compound on atherosclerosis is determined by measuring neointima formation following vascular injury.

-77-

9. The method of screening compounds as claimed in claim 6, wherein determining the effect of said compound on atherosclerosis is determined by measuring the rate of endothelial regeneration following vascular injury.

10. The method of screening compounds as claimed in claim 6, wherein said transgenic non-human animal has a disrupted apoE gene.

11. A method of screening compounds for potential utility to treat a vascular endothelial disorder comprising:

(a) providing a transgenic non-human animal having a disrupted endothelial nitric oxide synthase gene;

10 (b) administering a compound to be tested to said transgenic animal;

(c) determining the effect of said compound on said vascular endothelial disorder in said animal; and

(d) correlating the effect of said compound on said vascular endothelial disorder in said animal with a potential utility to treat said vascular endothelial disorder;

15 wherein said compound is not a NOS inhibitor.

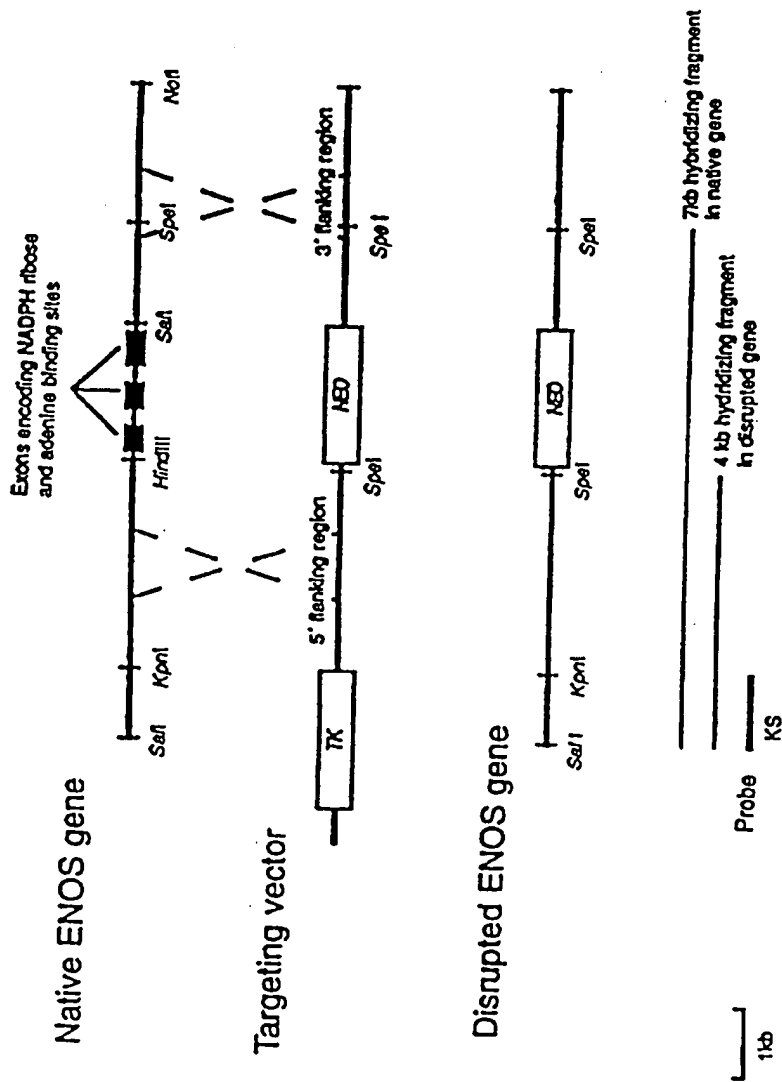
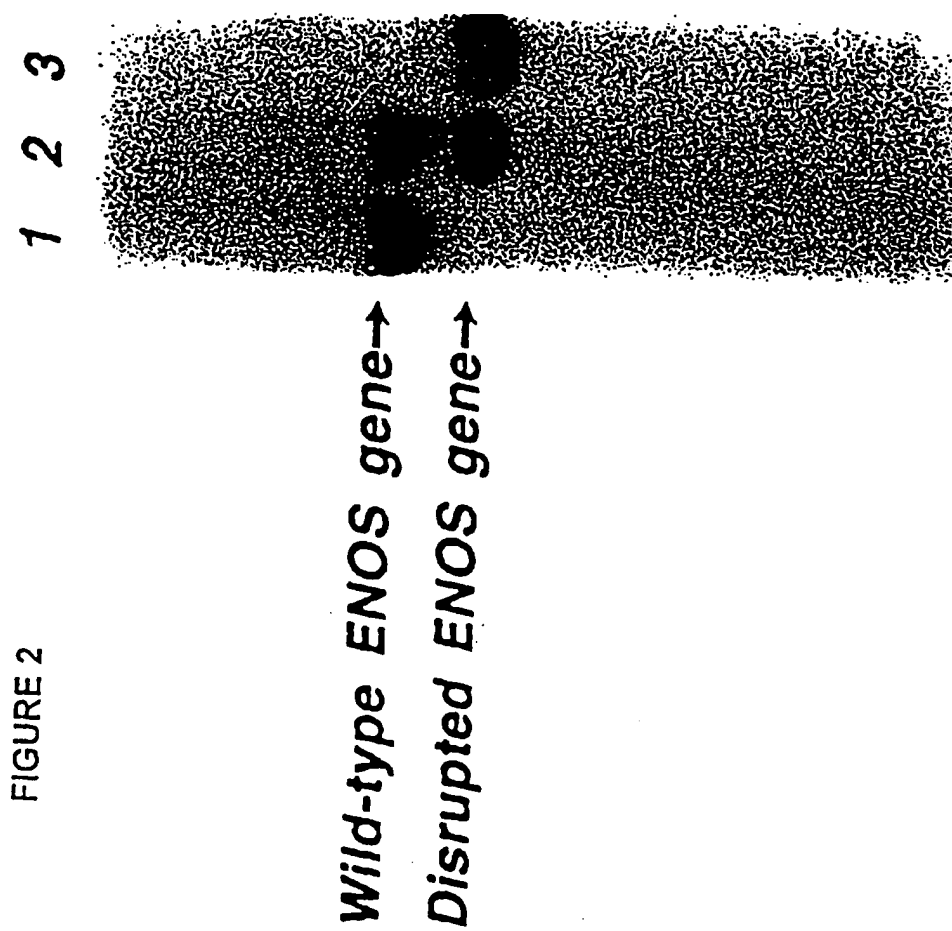


FIGURE 1





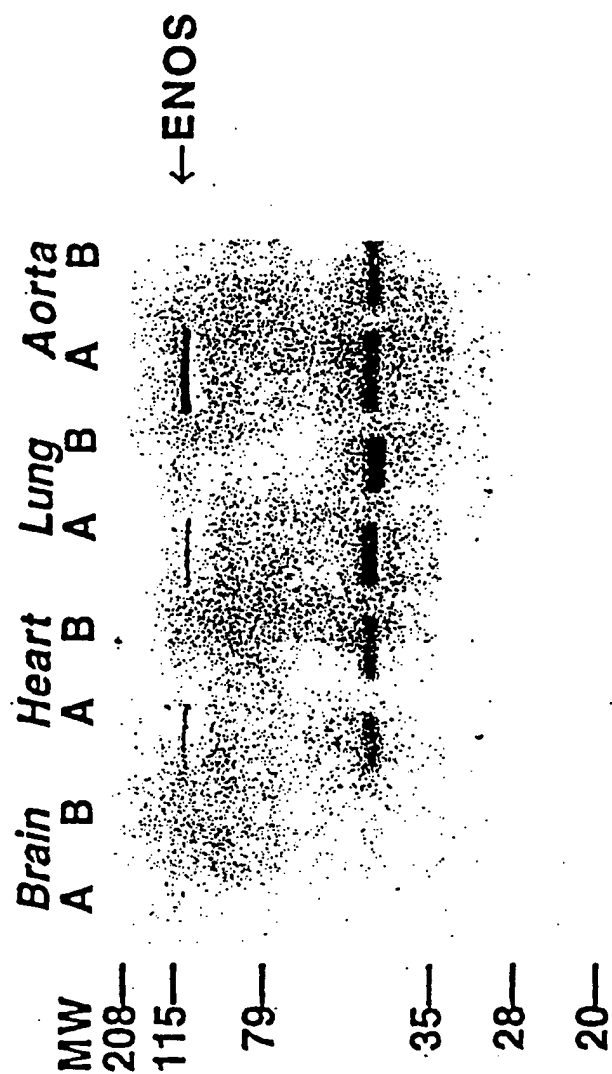


FIGURE 3

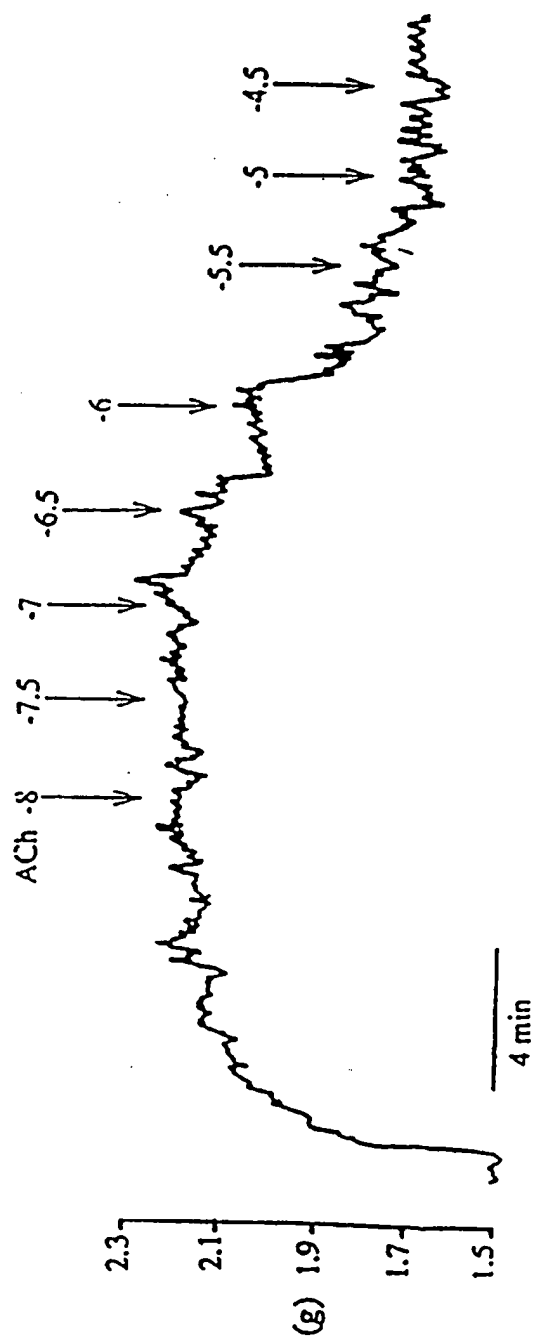


FIGURE 4A

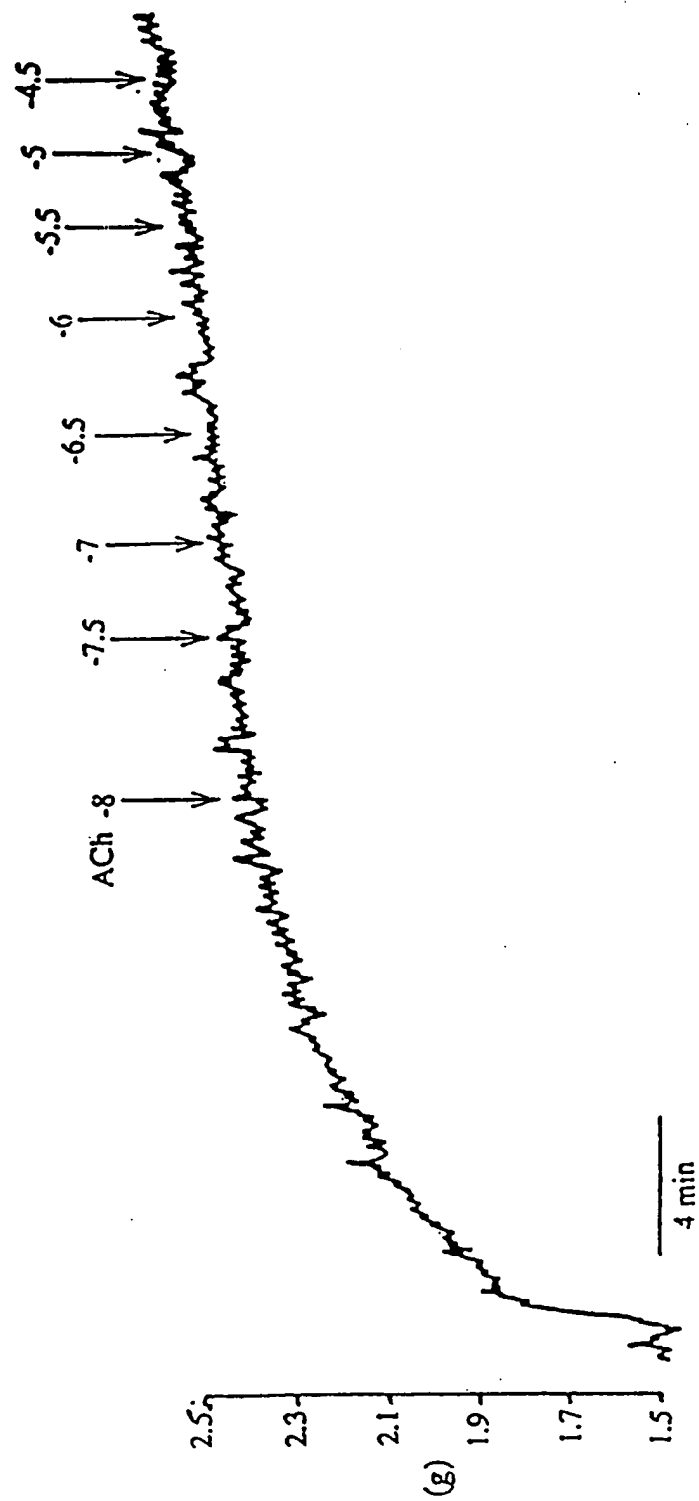


FIGURE 4B

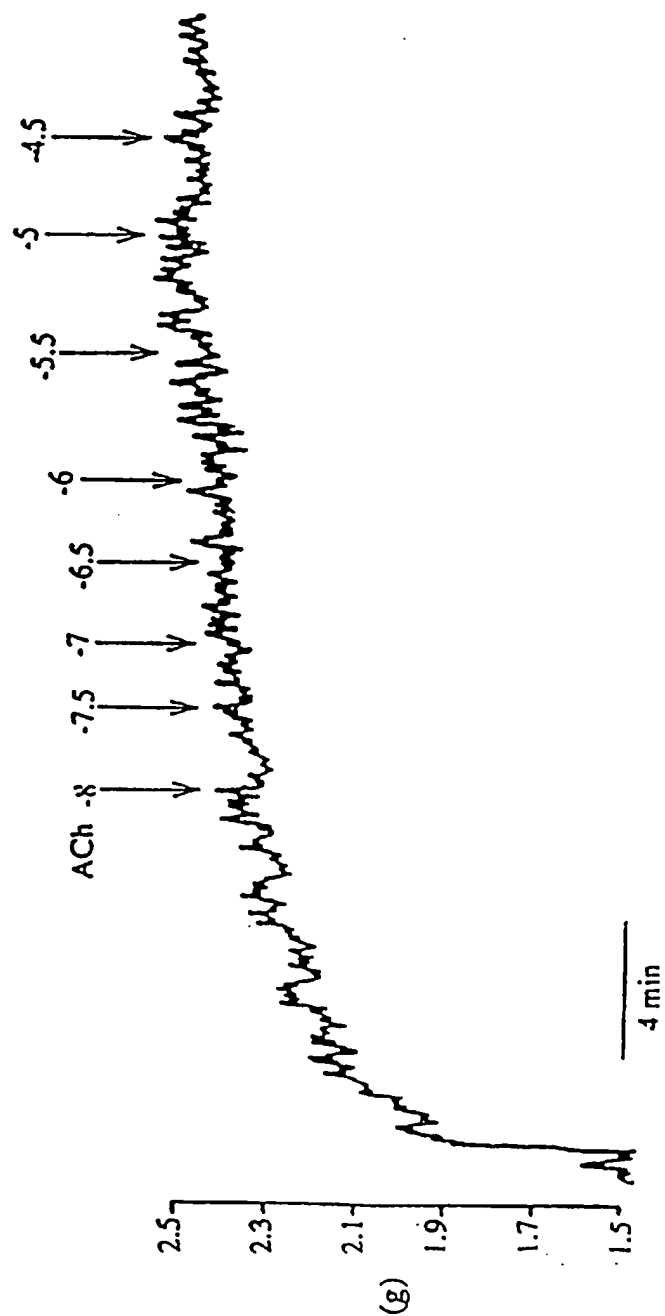


FIGURE 4C

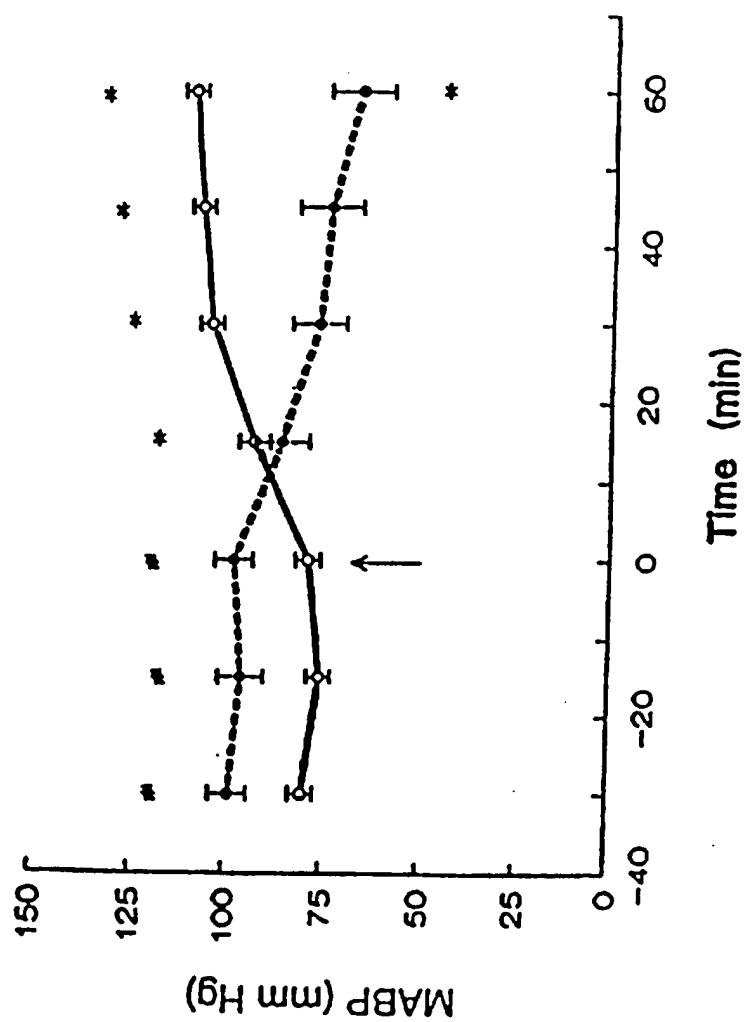
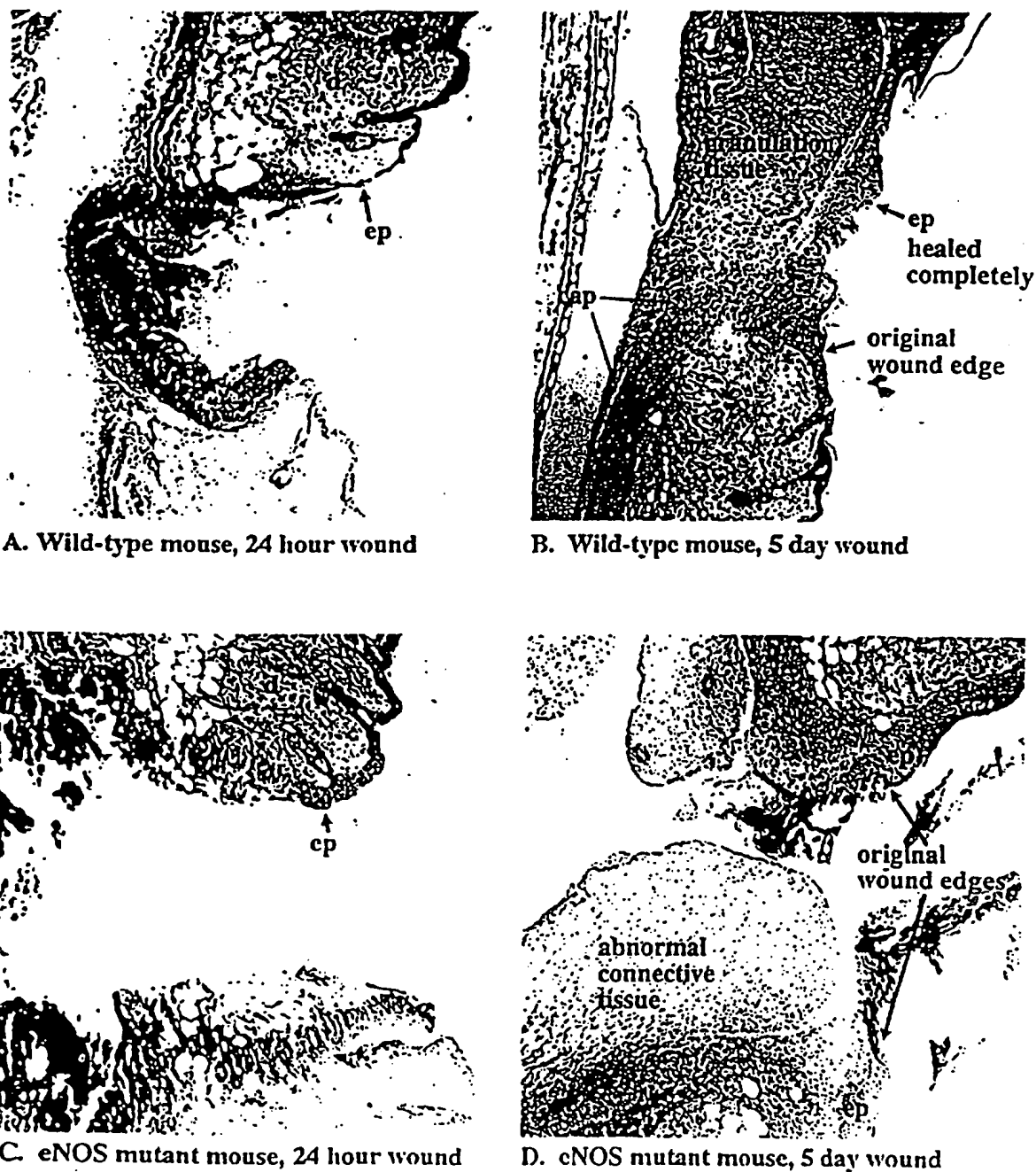


FIGURE 5

**FIGURE 6. WOUND HEALING IS ABNORMAL IN eNOS MUTANT MICE****Wound healing in eNOS mutant mice**

Wounds taken at 24 hours and 5 days. Wild-type wound has healed by 5 days. eNOS mutant wound does not heal, and demonstrates defective neovascularization. Details are described in the text.

FIGURE 7A

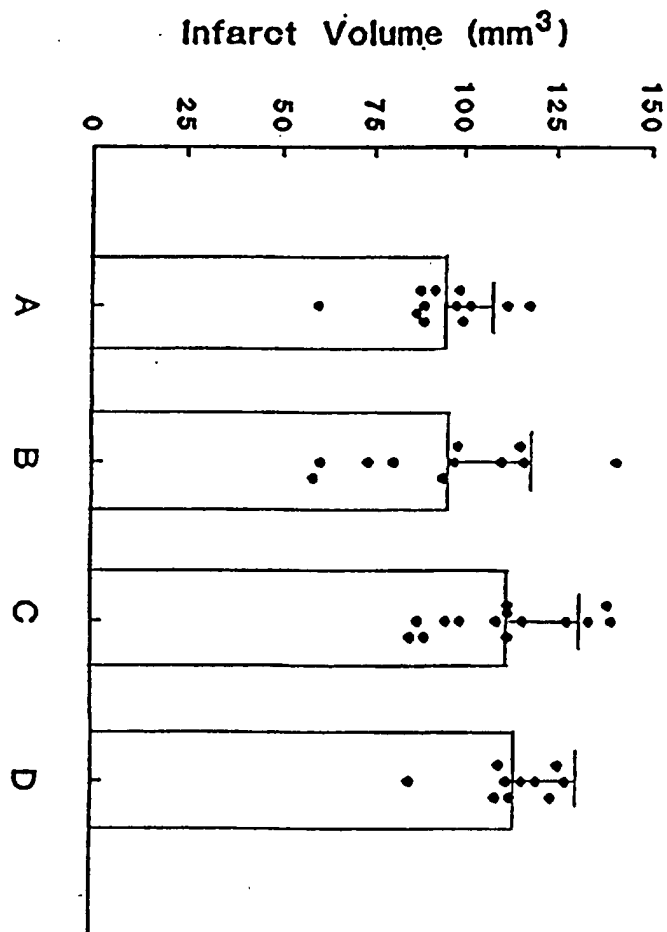




FIGURE 7B

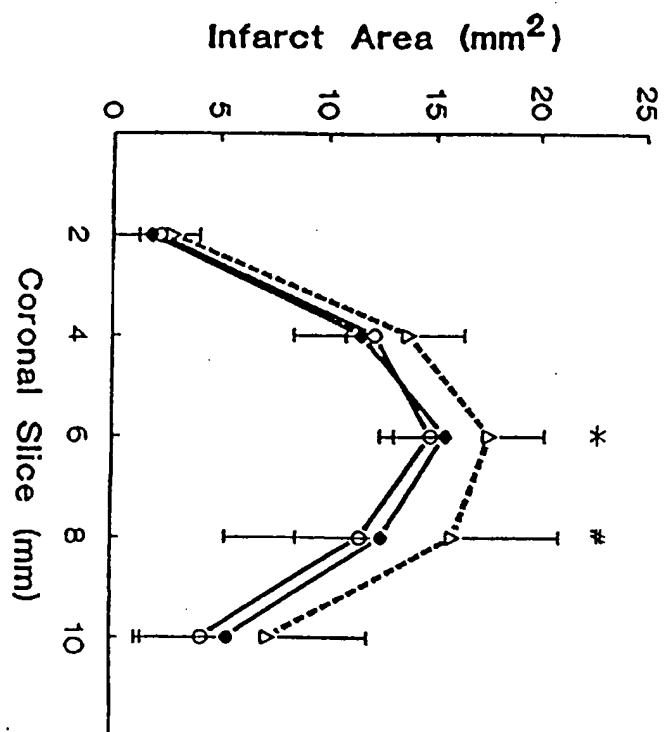
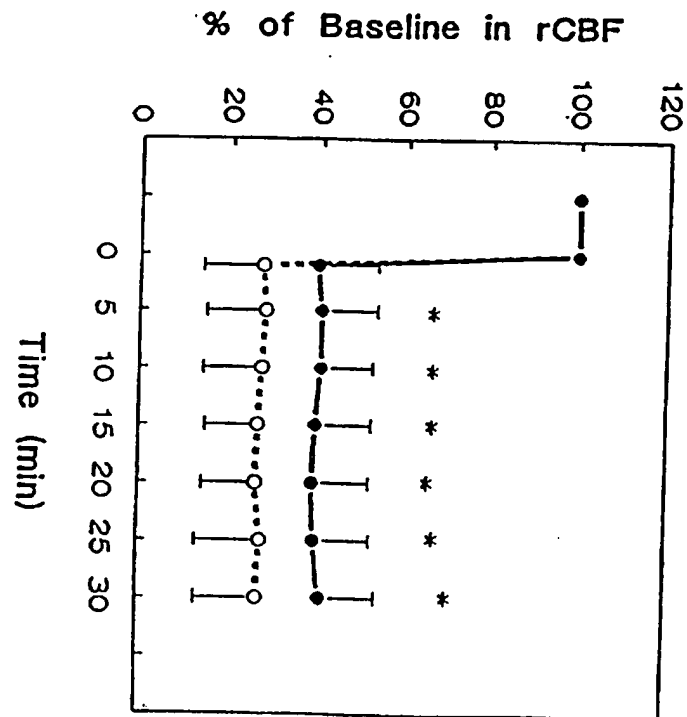


FIGURE 8



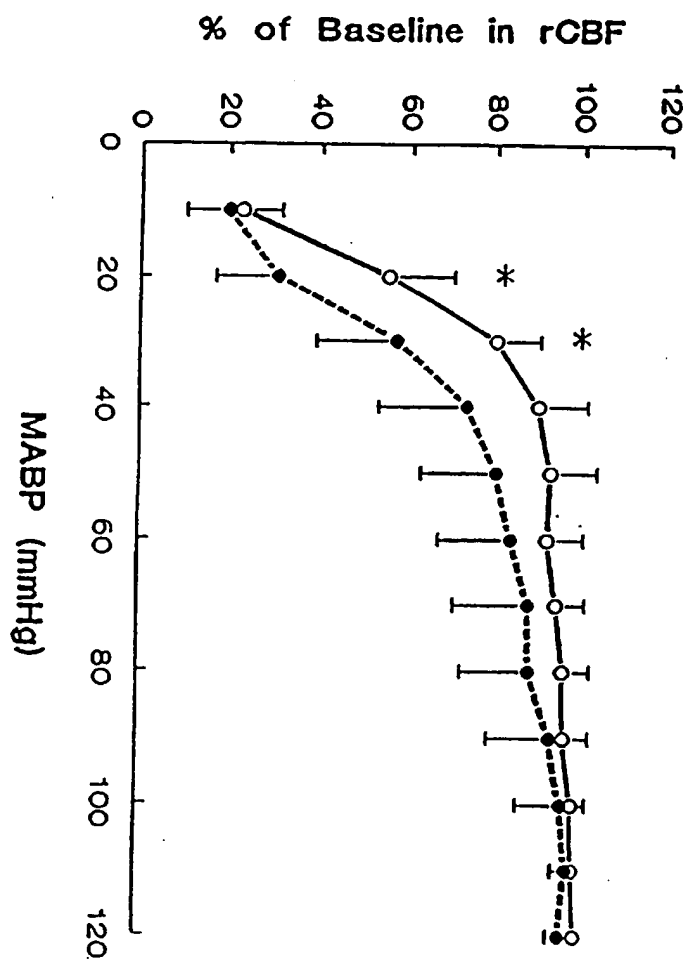
12/23  
FIGURE 9

FIGURE 10

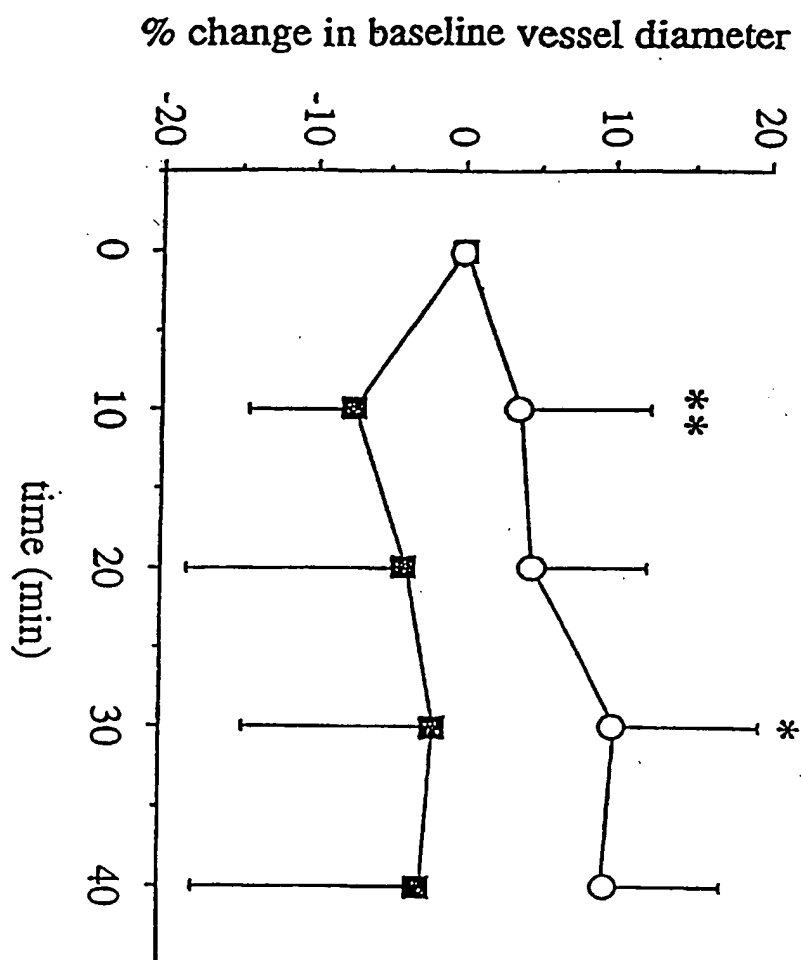




FIGURE 12

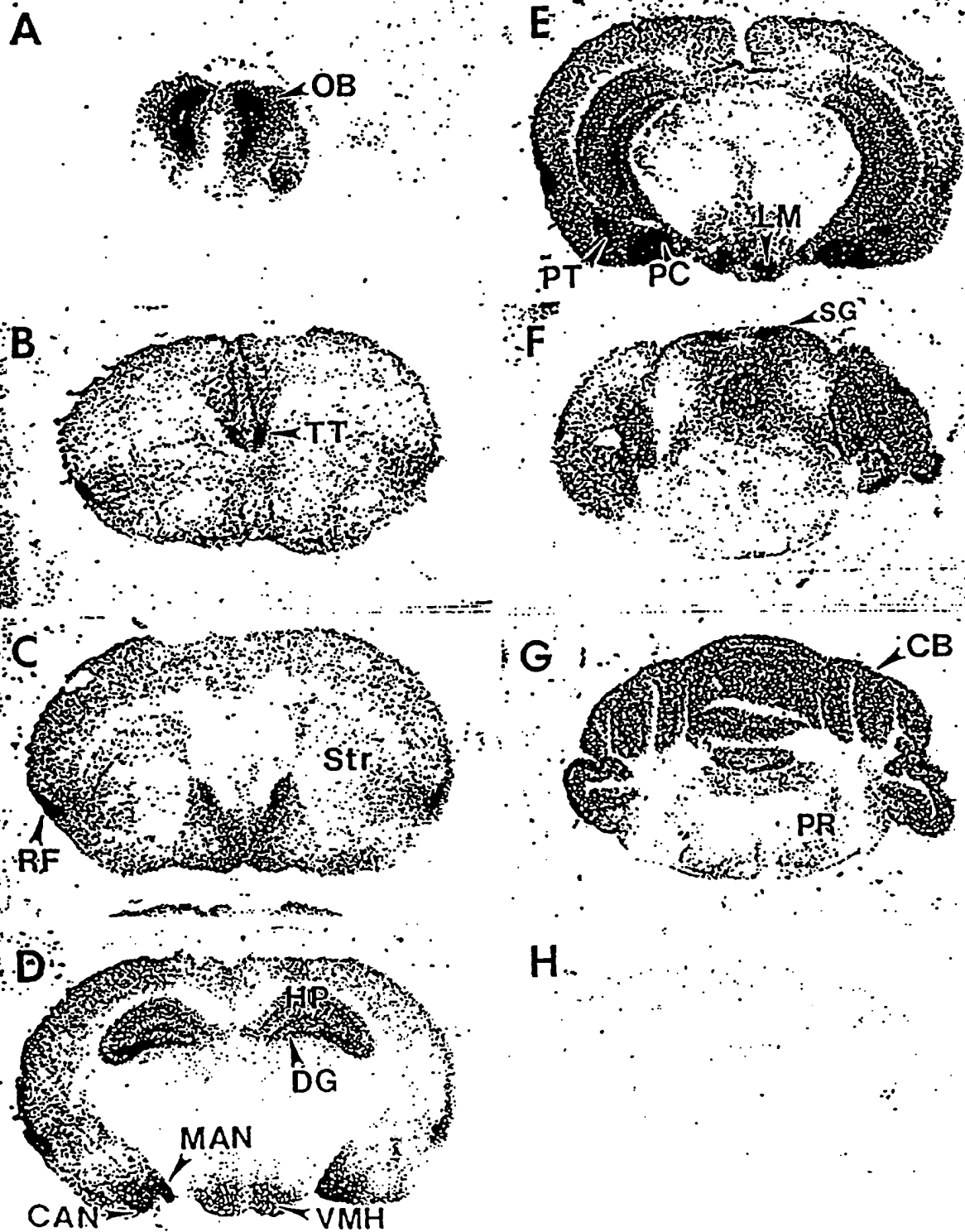


FIGURE 13

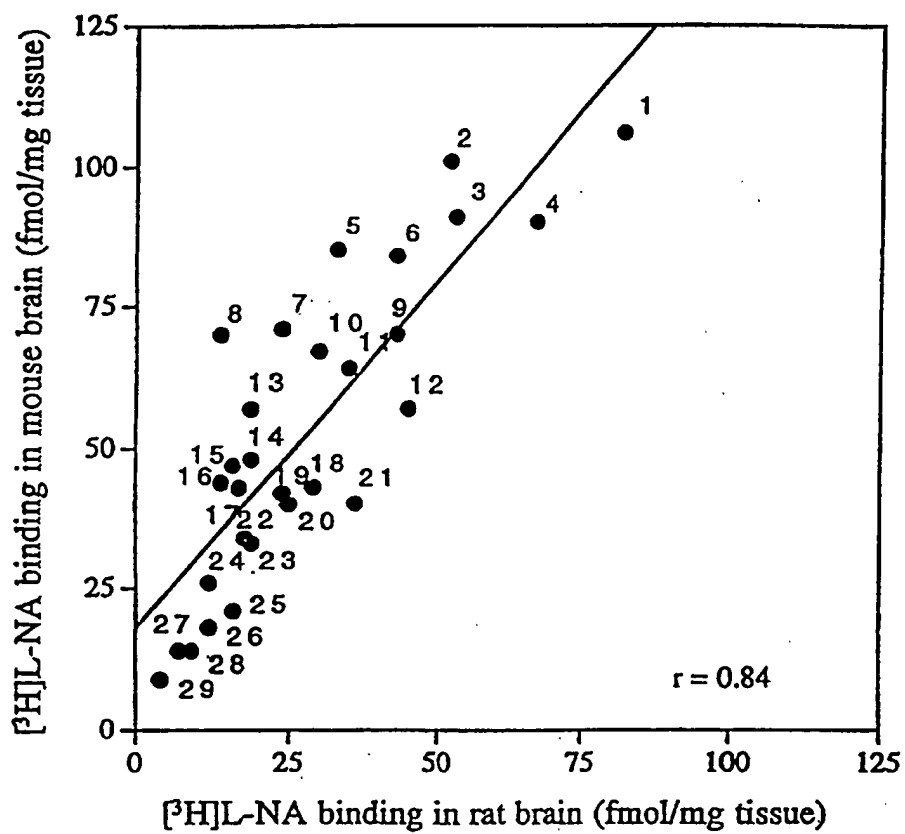
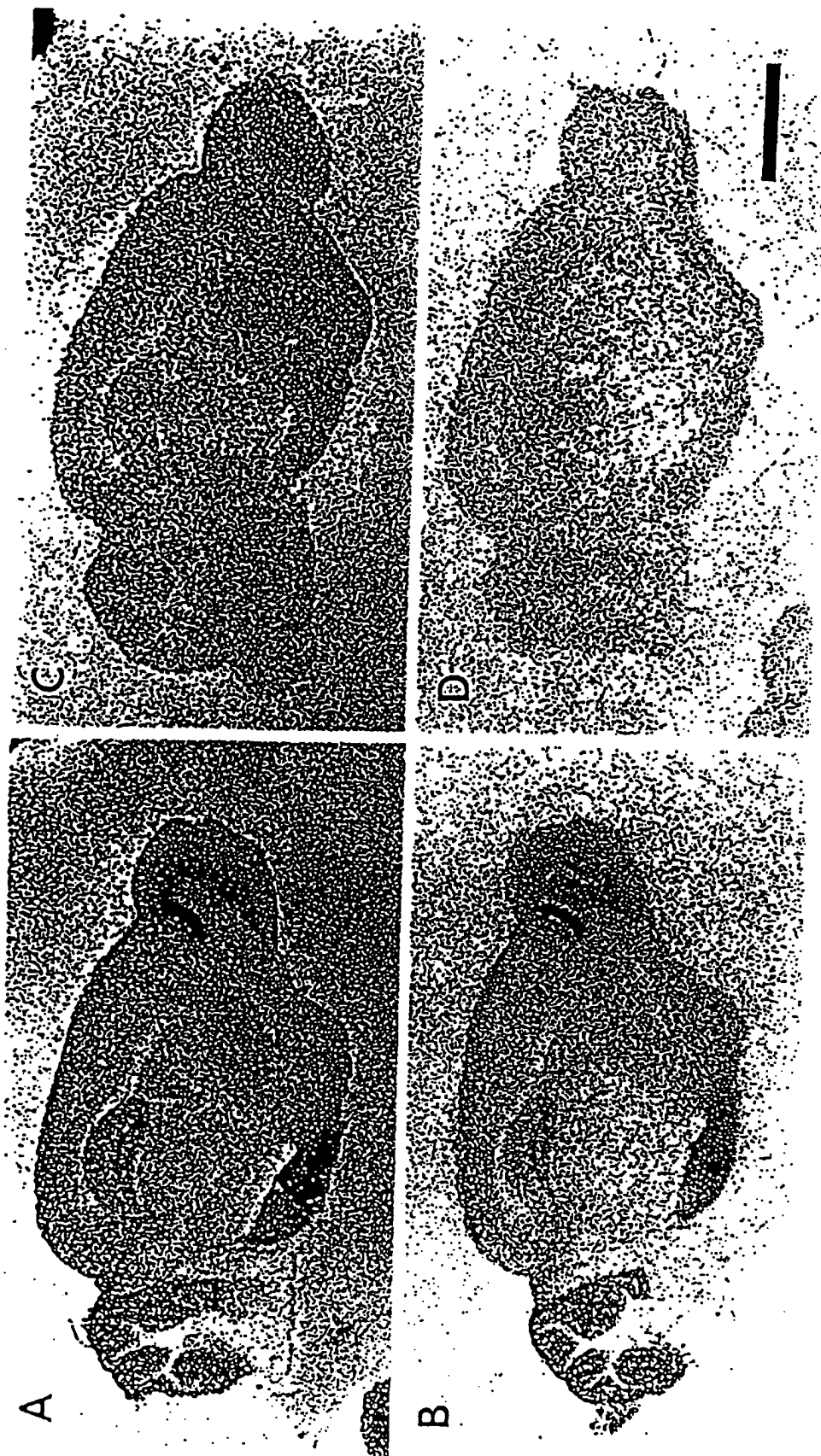
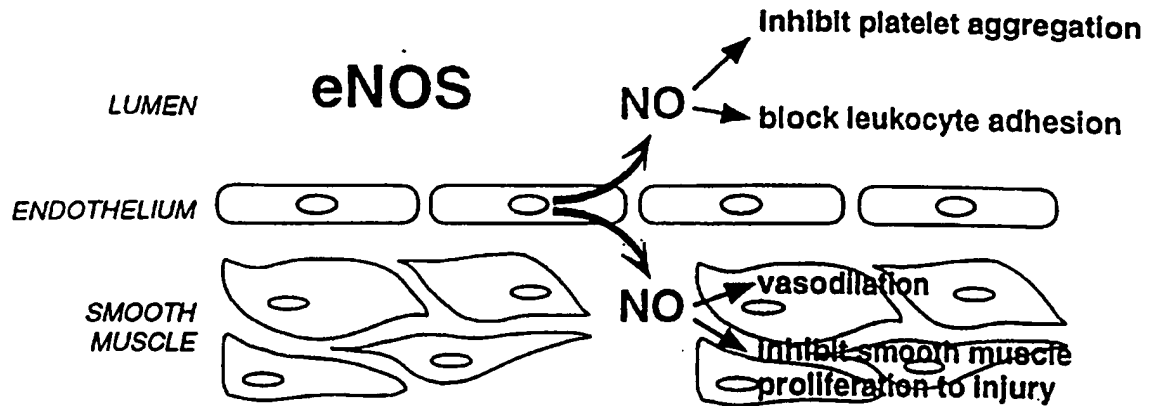


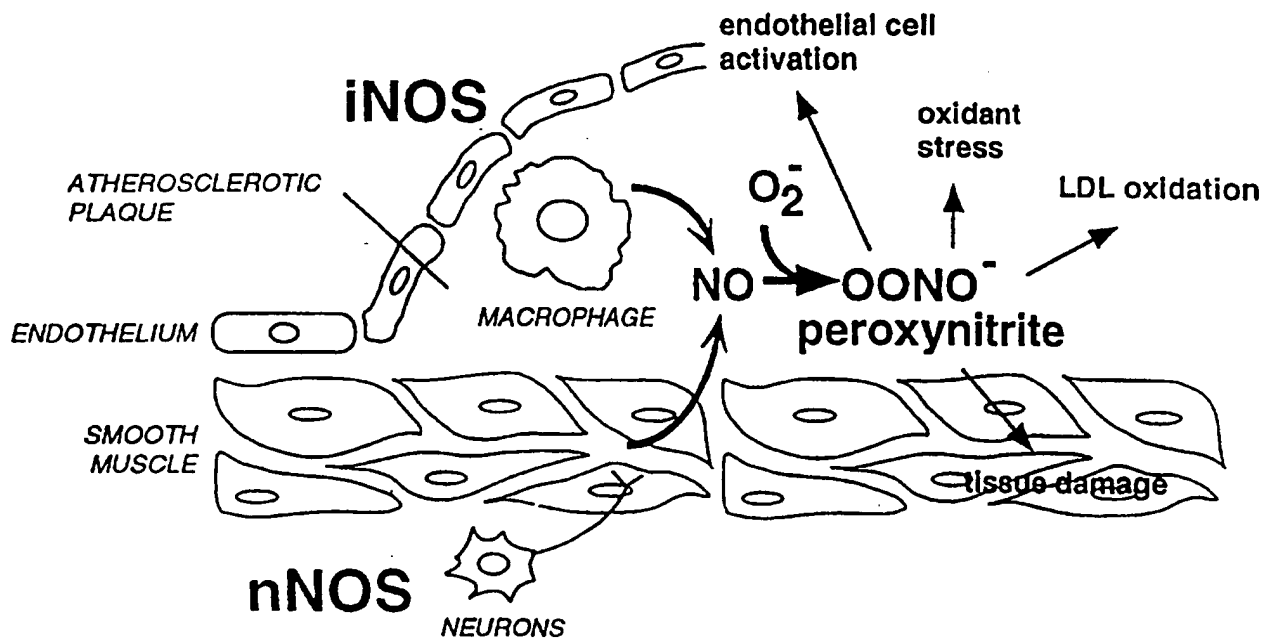
FIGURE 14







A. NO produced by normal vessels prevents proliferative response to injury and suppresses development of atherosclerosis



B. NO production in atherosclerotic plaques may lead to peroxynitrite formation, lipid oxidation, and endothelial cell activation

Figure 15 Effects of NO in normal and atherosclerotic arteries.

19/23

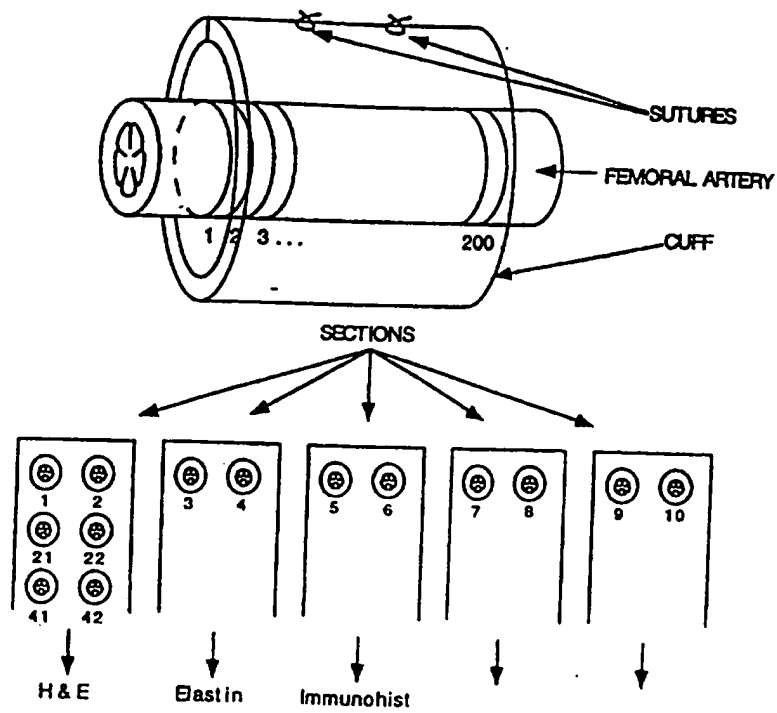
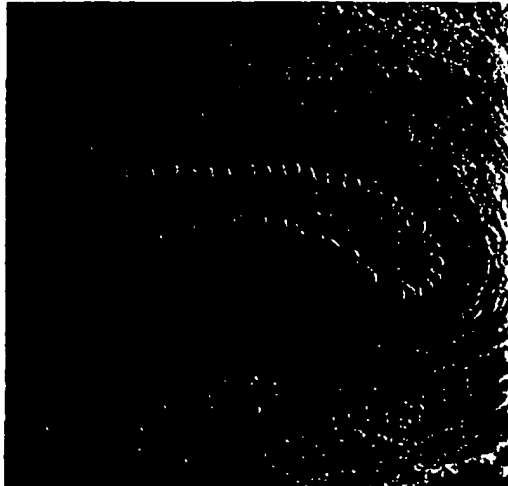


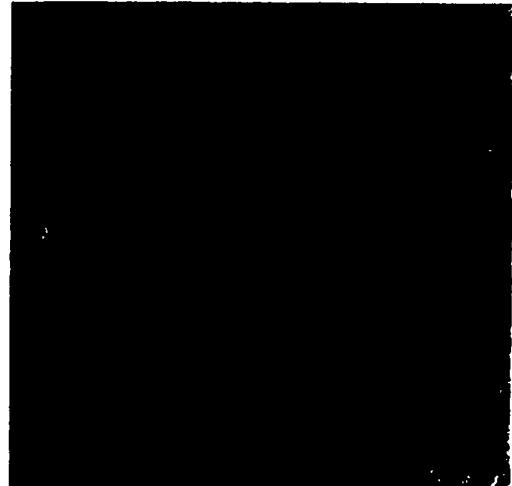
Figure 16

20/23

## H &amp; E stained sections of cuff-injured vessels



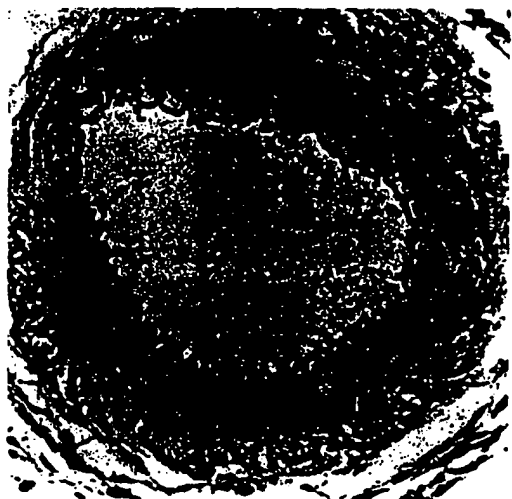
A. Wild-type vessel, injured



B. Wild-type vessel, control



C. eNOS mutant vessel, injured



D. eNOS mutant vessel, control

*Figure 17* Hematoxylin and eosin stained sections of cuff-injured vessels. Injured vessels contain neointima seen inside of the internal elastic lamina (shown with arrows). Control vessels do not. eNOS mutant mice show significantly increased neointimal formation, shown with asterisk (\*).



Figure 18 Histology and immunochemical staining of injured and control vessels from eNOS mutant mice. Note the position of the internal elastic lamina in each section. Control vessels have no intima.

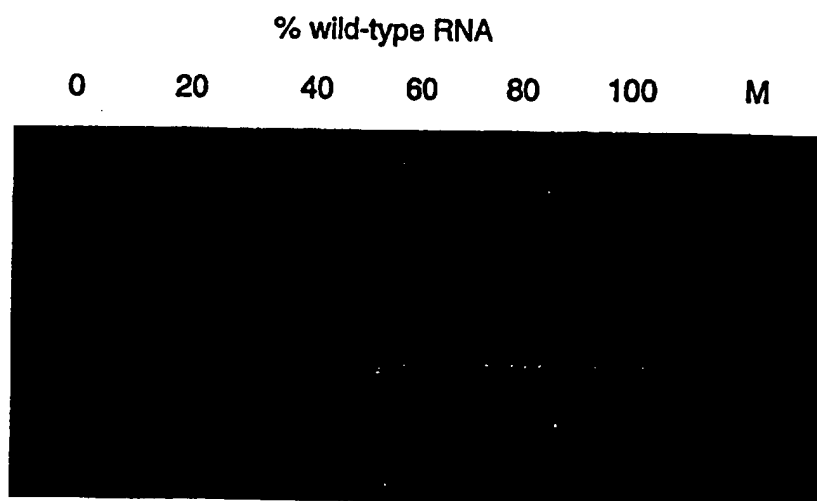


Figure 19. Quantitative RT-PCR of eNOS mRNA from mouse aorta



A



B



C



D

*Figure 20* Atherosclerotic lesions from apoE mutant mice at 6 months.  
 A. Aortic arch and carotid arteries. B. Thoracic aorta. C. Descending thoracic aorta. D. Oil red O stain of an aortic lesion.

# INTERNATIONAL SEARCH REPORT

Inter. Application No

PCT/US 97/04184

## A. CLASSIFICATION OF SUBJECT MATTER

IPC 6 C12N15/00 A01K67/027 C12N9/02 C12N15/53

According to International Patent Classification (IPC) or to both national classification and IPC

## B. FIELDS SEARCHED

Minimum documentation searched (classification system followed by classification symbols)

IPC 6 A01K C12N

Documentation searched other than minimum documentation to the extent that such documents are included in the fields searched

Electronic data base consulted during the international search (name of data base and, where practical, search terms used)

## C. DOCUMENTS CONSIDERED TO BE RELEVANT

Category *	Citation of document, with indication, where appropriate, of the relevant passages	Relevant to claim No.
X	STROKE, vol. 27, no. 1, 25 January 1996, page 173 XP000607805 HUANG Z ET AL: "FOCAL CEREBRAL ISCHEMIA IN MICE DEFICIENT IN EITHER ENDOTHELIAL (ENOS) OR NEURONAL NITRIC OXIDE (NNOS) SYNTHASE" see abstract	1-4,6,11
X	NATURE, vol. 377, 21 September 1995, pages 239-242, XP002021109 HUANG P L ET AL: "HYPERTENSION IN MICE LACKING THE GENE FOR ENDOTHELIAL NITRIC OXIDE SYNTHASE" see abstract see page 241, column 1, paragraph 2	7-9,11

☒ Further documents are listed in the continuation of box C.

☒ Patent family members are listed in annex.

### \* Special categories of cited documents:

- \*A\* document defining the general state of the art which is not considered to be of particular relevance
- \*E\* earlier document but published on or after the international filing date
- \*L\* document which may throw doubts on priority claim(s) or which is cited to establish the publication date of another citation or other special reason (as specified)
- \*O\* document referring to an oral disclosure, use, exhibition or other means
- \*P\* document published prior to the international filing date but later than the priority date claimed

- \*T\* later document published after the international filing date or priority date and not in conflict with the application but cited to understand the principle or theory underlying the invention
- \*X\* document of particular relevance; the claimed invention cannot be considered novel or cannot be considered to involve an inventive step when the document is taken alone
- \*Y\* document of particular relevance; the claimed invention cannot be considered to involve an inventive step when the document is combined with one or more other such documents, such combination being obvious to a person skilled in the art
- \*Z\* document member of the same patent family

Date of the actual completion of the international search

26 June 1997

Date of mailing of the international search report

11.07.97.

Name and mailing address of the ISA

European Patent Office, P.B. 5818 Patentaan 2  
NL - 2280 HV Rijswijk  
Tel. (+31-70) 340-2040, Tx. 31 651 epo nl,  
Fax (+31-70) 340-3016

Authorized officer

Chambonnet, F

# INTERNATIONAL SEARCH REPORT

International Application No.  
PCT/US 97/04184

## C.(Continuation) DOCUMENTS CONSIDERED TO BE RELEVANT

Category *	Citation of document, with indication, where appropriate, of the relevant passages	Relevant to claim No.
A	WO 93 19166 A (UNIV NORTH CAROLINA) 30 September 1993 see the whole document ---	10
P,X	CIRCULATION, vol. 94, no. 8 sup, 15 October 1996, page 1154 XP000676824 MOROI, M. ET AL.: "Mice mutant in endothelial Nitric Oxide synthase: vessel growth and response to injury" see abstract ---	8,9,11
P,X	AMERICAN JOURNAL OF PHYSIOLOGY, vol. 272, no. 3 pt 2, March 1997, page h1401 XP000676924 HUANG, Z. ET AL.: "bFGF ameliorates focal ischemic injury by blood flow-independent mechanisms in eNOS mutant mice" see the whole document ---	1
T	JOURNAL OF MOLECULAR MEDICINE, vol. 74, no. 8, 1996, pages 415-421, XP000610408 HUANG P L ET AL: "GENETIC ANALYSIS OF NITRIC OXIDE SYNTHASE ISOFORMS: TARGETED MUTATION IN MICE" see the whole document -----	1



information on patent family members

PCT/US 97/04184

Form PCT/ISA/210 (patent family annex) (July 1992)

**This Page is Inserted by IFW Indexing and Scanning  
Operations and is not part of the Official Record**

**BEST AVAILABLE IMAGES**

Defective images within this document are accurate representations of the original documents submitted by the applicant.

Defects in the images include but are not limited to the items checked:

- ☐ BLACK BORDERS
- ☐ IMAGE CUT OFF AT TOP, BOTTOM OR SIDES
- ☐ FADED TEXT OR DRAWING
- ☒ BLURRED OR ILLEGIBLE TEXT OR DRAWING
- ☐ SKEWED/SLANTED IMAGES
- ☐ COLOR OR BLACK AND WHITE PHOTOGRAPHS
- ☐ GRAY SCALE DOCUMENTS
- ☒ LINES OR MARKS ON ORIGINAL DOCUMENT
- ☐ REFERENCE(S) OR EXHIBIT(S) SUBMITTED ARE POOR QUALITY
- ☐ OTHER: \_\_\_\_\_

**IMAGES ARE BEST AVAILABLE COPY.**

**As rescanning these documents will not correct the image problems checked, please do not report these problems to the IFW Image Problem Mailbox.**